A novel series of tetrahydrothieno[2,3-c]pyridin-2-yl derivatives: Fluorescence Spectroscopy and BSA Binding, ADMET properties, Molecular Docking, and DFT studies

Goncagül Serdaroğlu[1,*], Nesimi Uludag[2], Elvan Üstün[3], Naki Colak[4]

[1]Sivas Cumhuriyet University, Faculty of Education, Math. and Sci. Edu., 58140, Sivas, Turkey;
e-mail:goncagul.serdaroglu@gmail.com
[2]Department of Chemistry, Faculty of Arts and Sciences, Namık Kemal University, 59030, Tekirdağ, Turkey;
e-mail: nuludag@nku.edu.tr
[3]Department of Chemistry, Faculty of Art and Science, Ordu University, 52200 Ordu, Turkey,
e-mail: elvanustun@odu.edu.tr
[4]Department of Chemistry, Hitit University, Department of Chemistry, Corum 19030, Turkey,
e-mail: nakicolak@hitit.edu.tr

Table of Contents

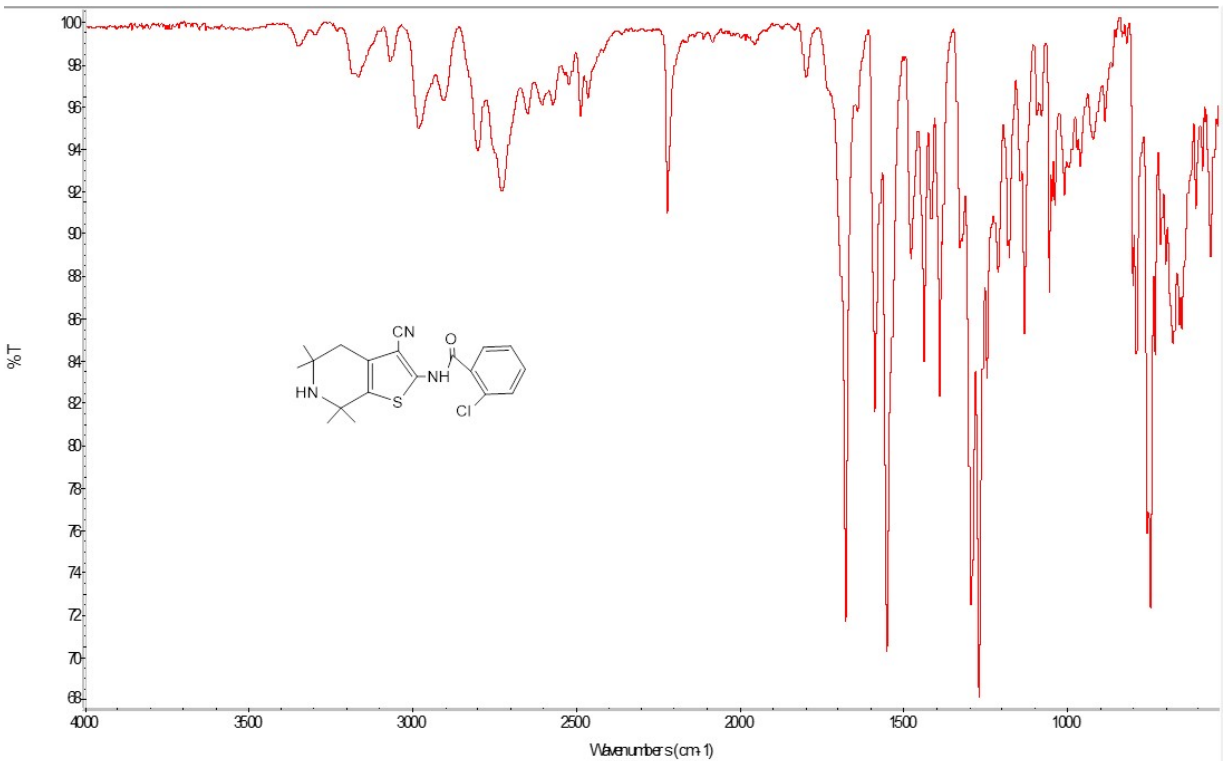

Fig. S1a. The recorded *FT-IR* spectrum of the compound **C1**

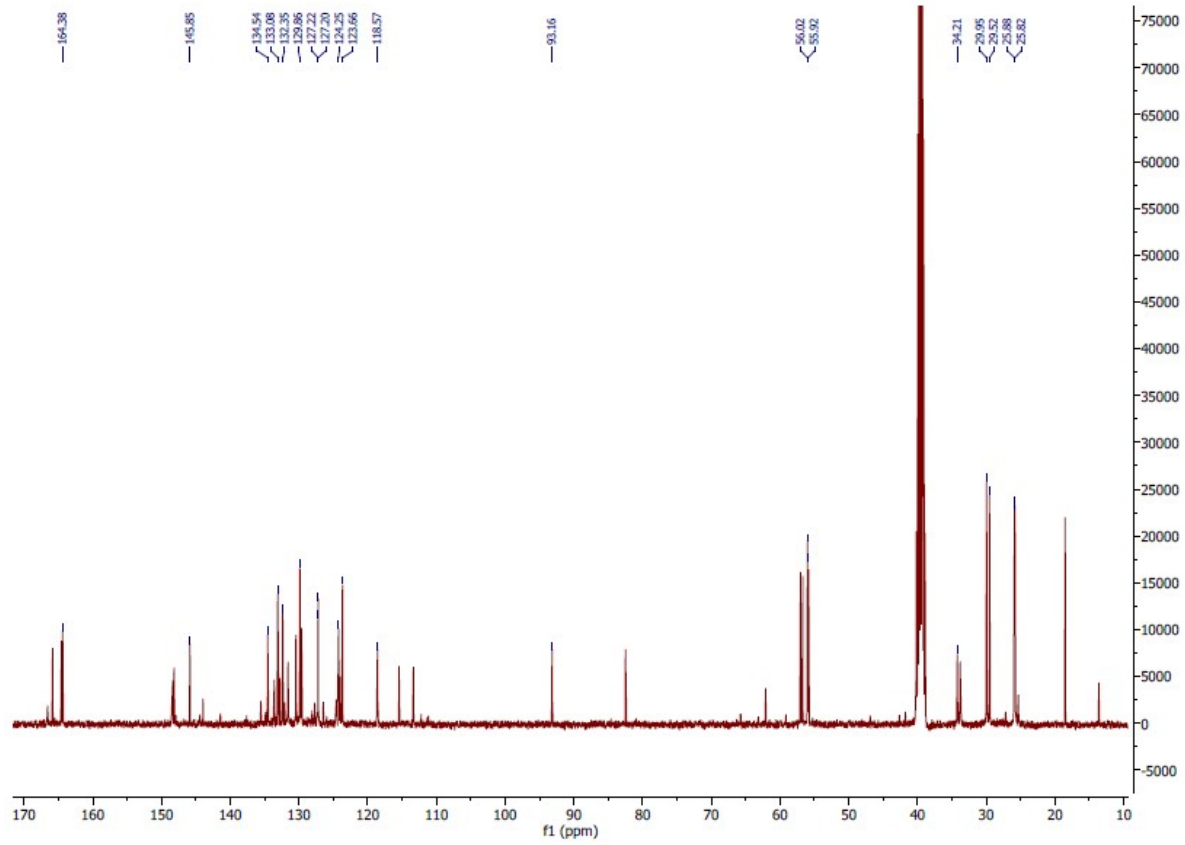

Fig. S1b. The recorded *^{13}C NMR* spectrum of the compound **C1**

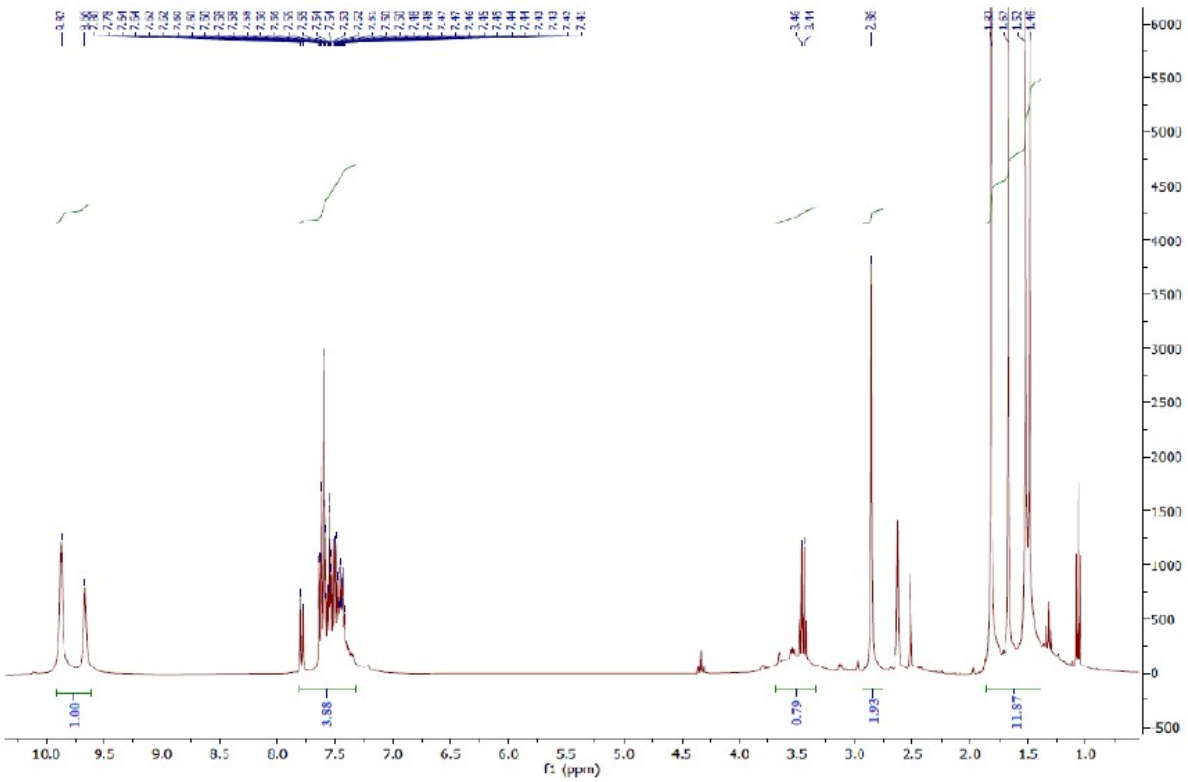

Fig. S1c. The recorded *^{1}H NMR* spectrum of the compound **C1**

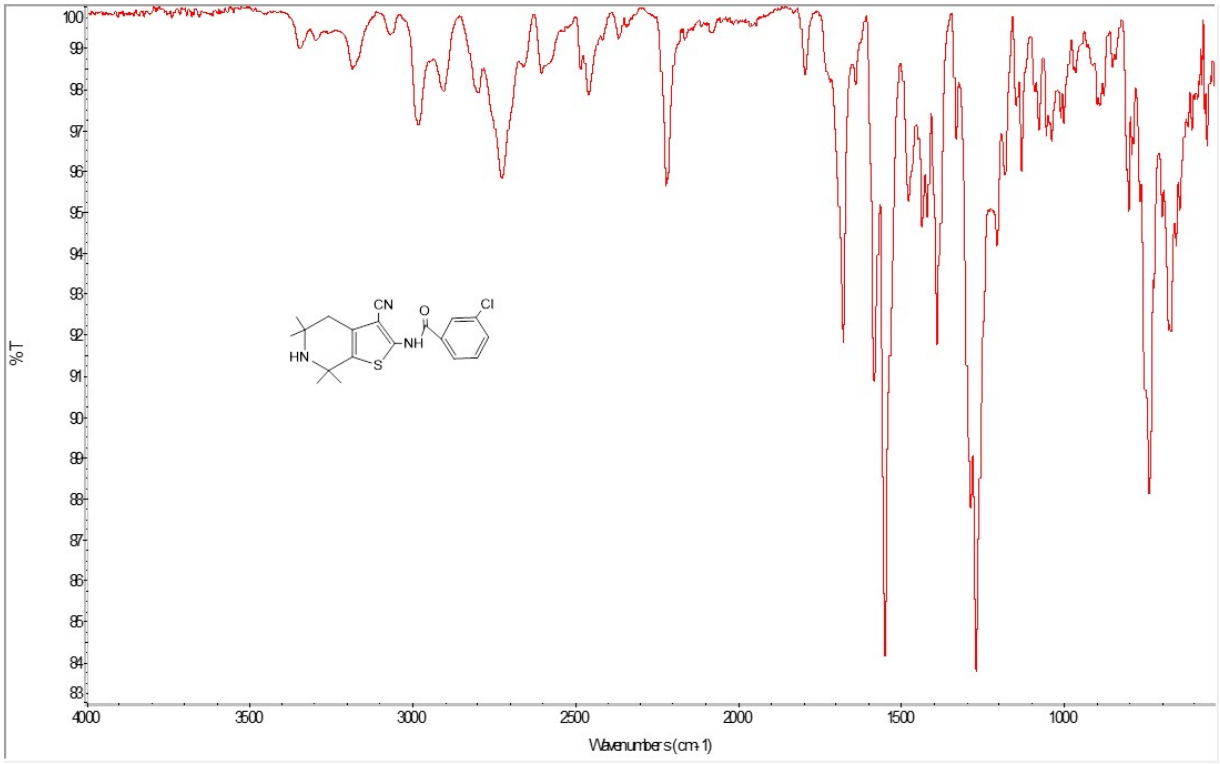

Fig. S2a. The recorded *FT-IR* spectrum of the compound **C2**

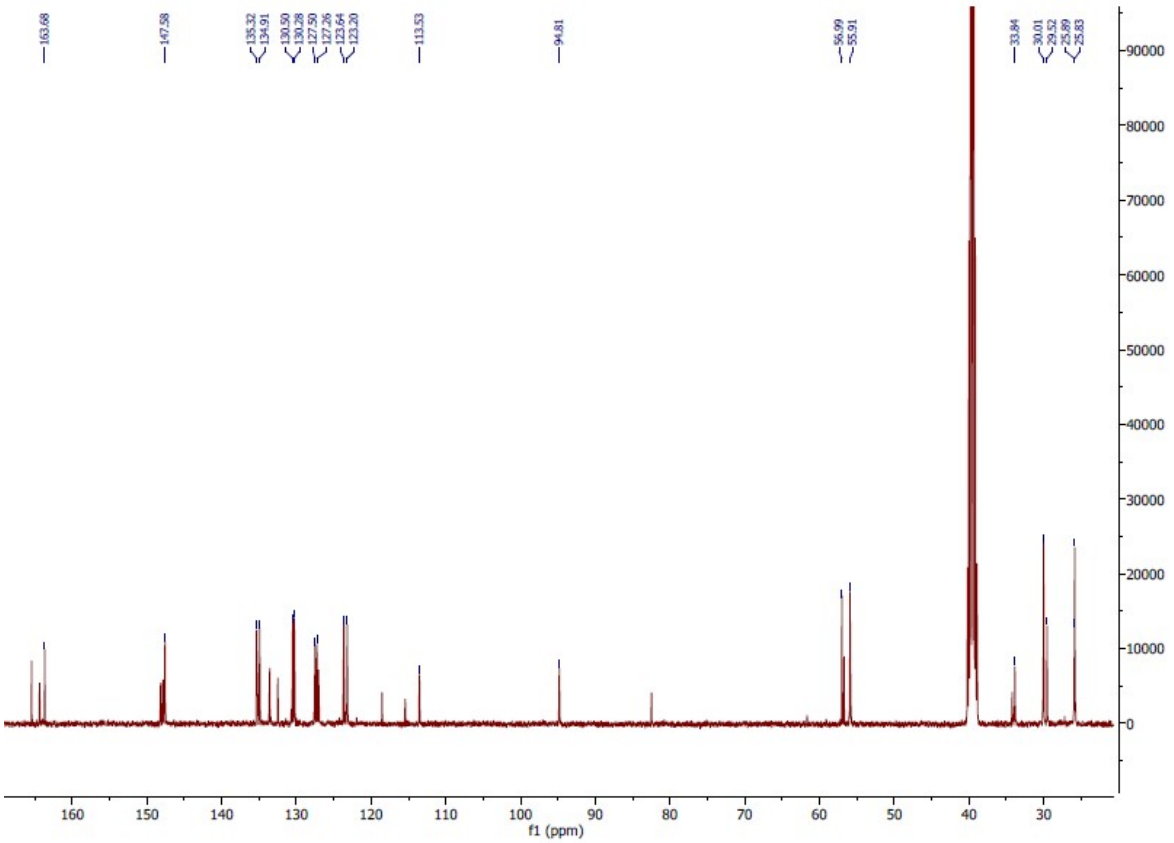

Fig. S2b. The recorded *^{13}C NMR* spectrum of the compound **C2**

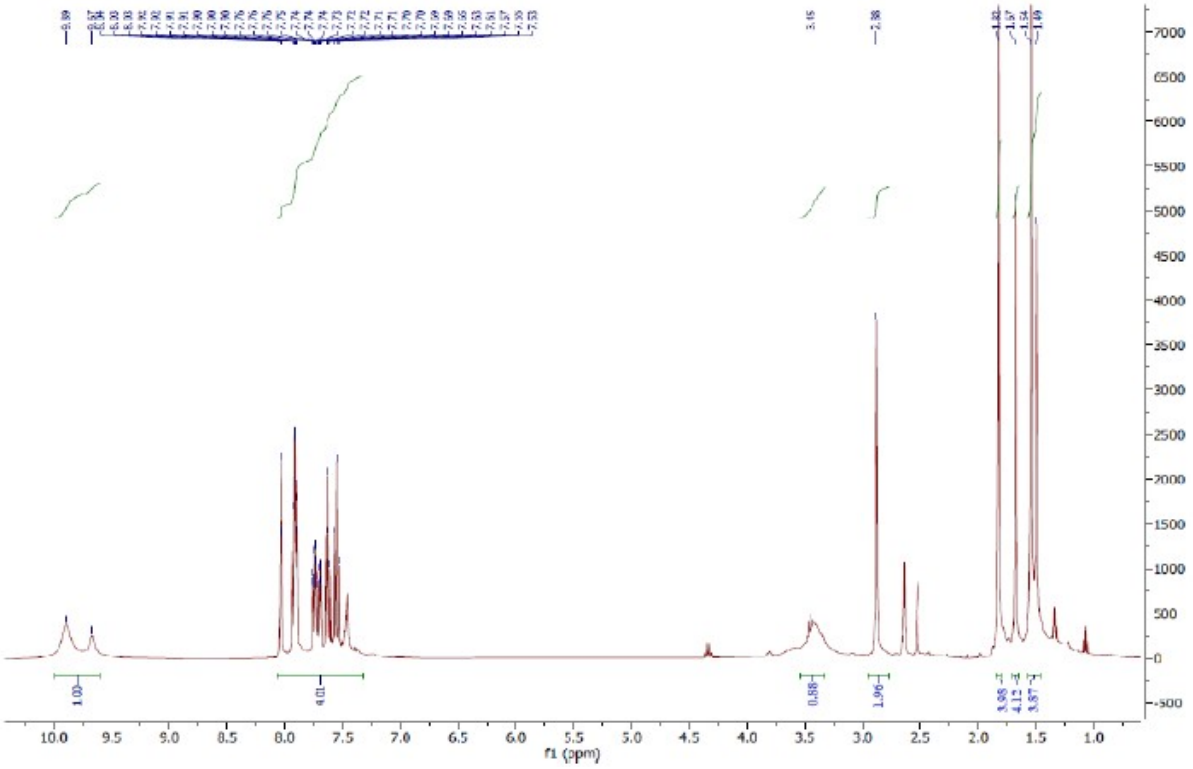

Fig. S2c. The recorded *^{1}H NMR* spectrum of the compound **C2**

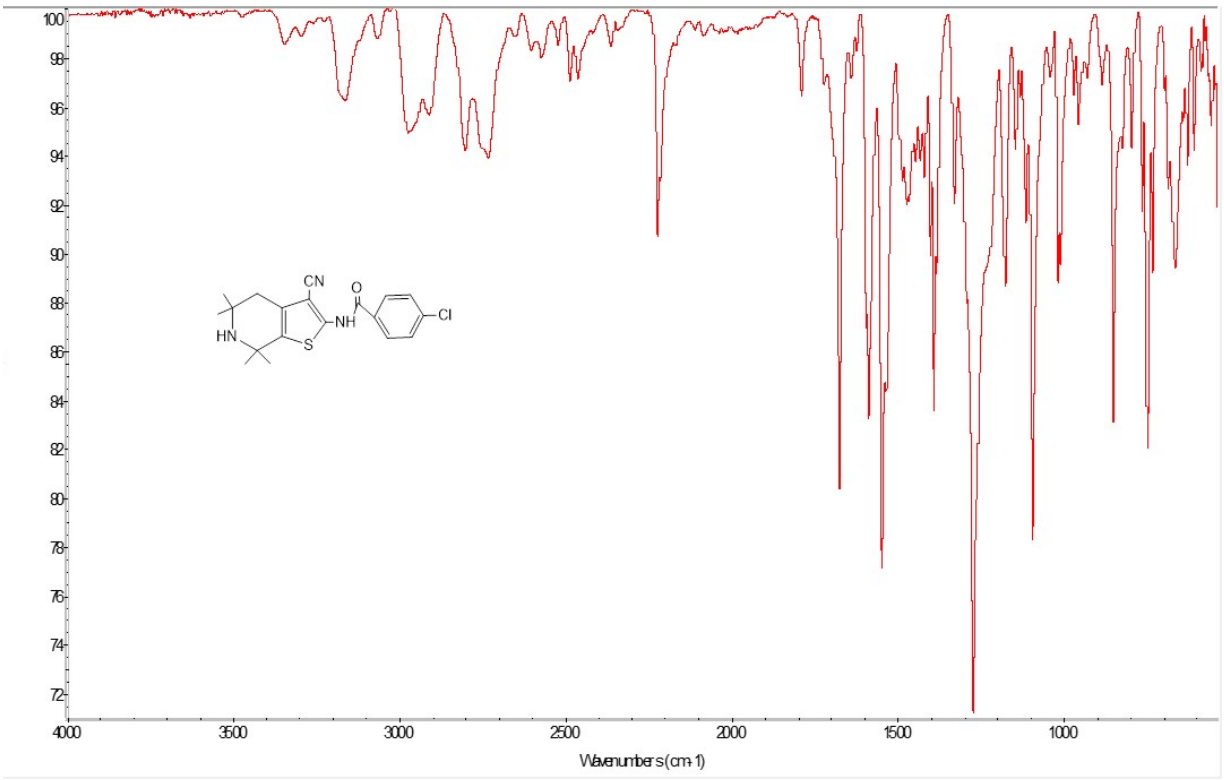

Fig. S3a. The recorded *FT-IR* spectrum of the compound **C3**

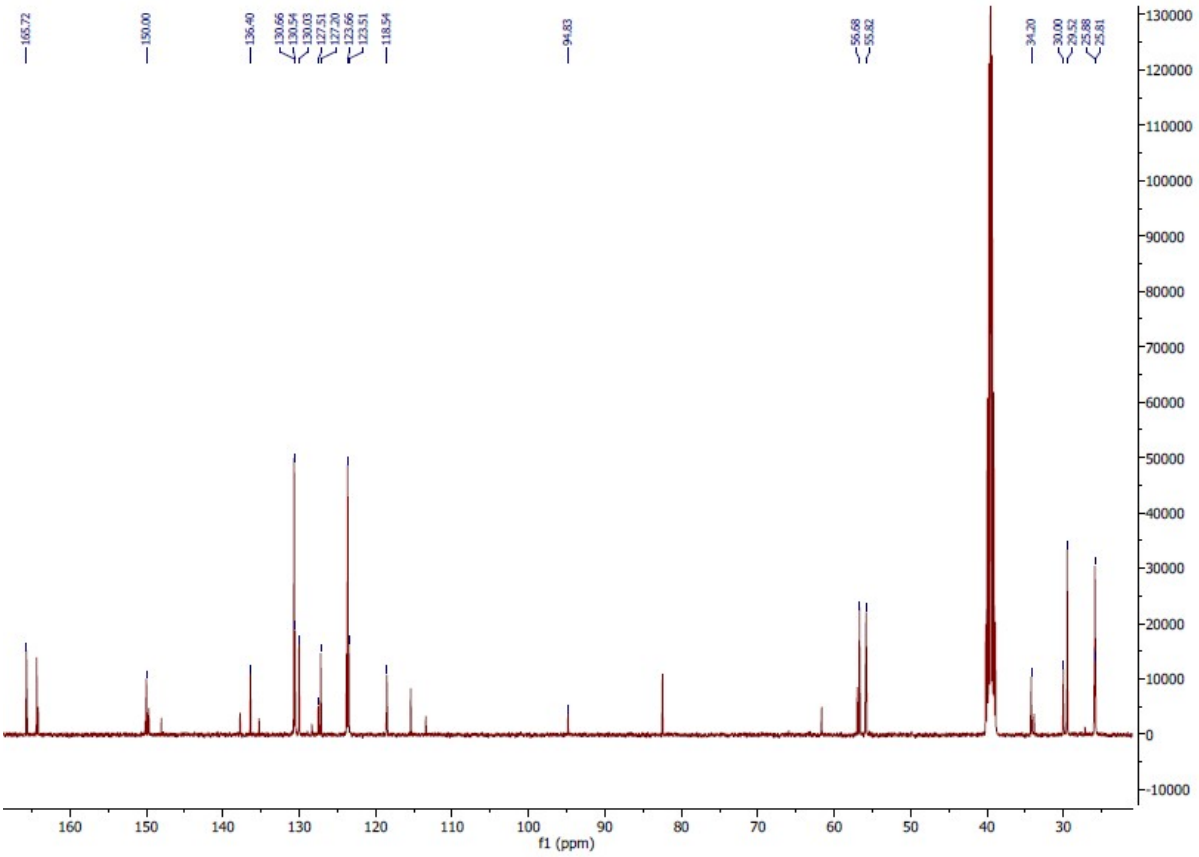

Fig. S3b. The recorded *^{13}C NMR* spectrum of the compound **C3**

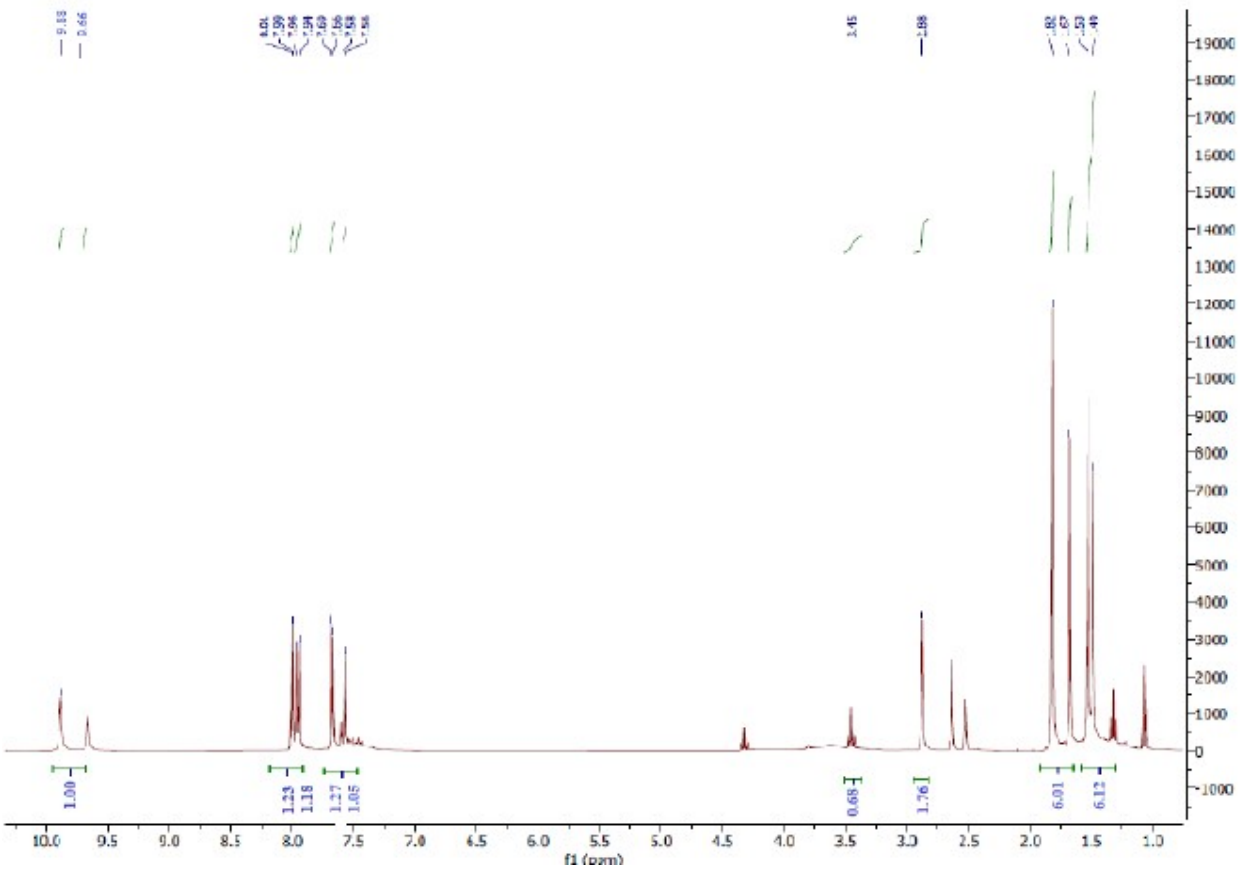

Fig. S3c. The recorded *^{1}H NMR* spectrum of the compound **C3**

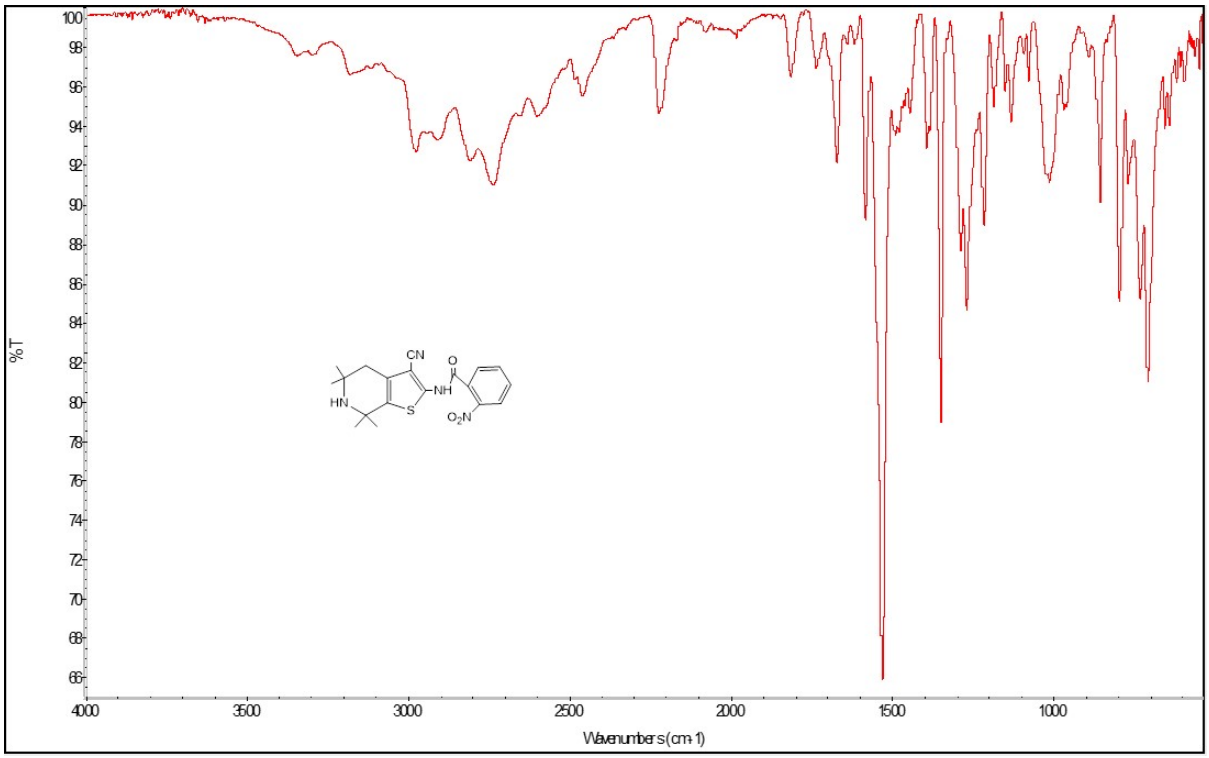

Fig. S4a. The recorded *FT-IR* spectrum of the compound **N1**

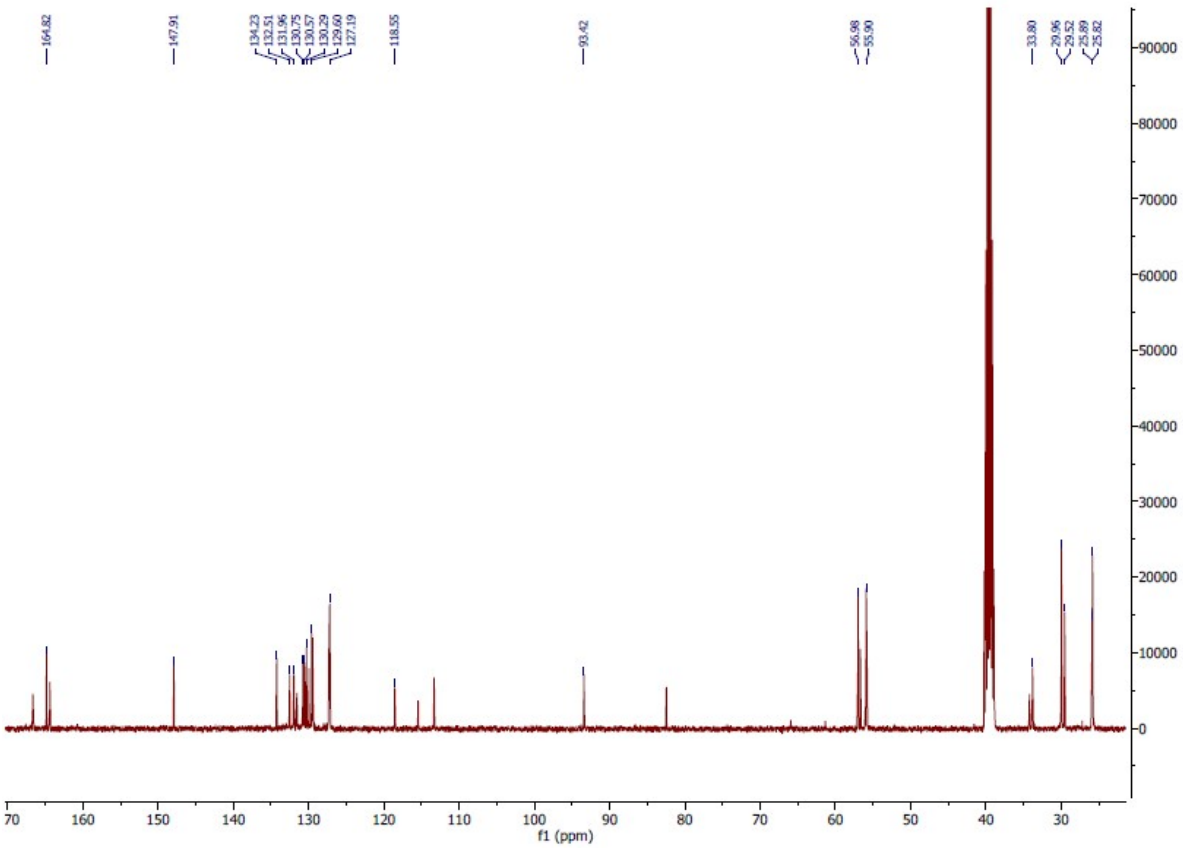

Fig. S4b. The recorded *[13]C NMR* spectrum of the compound **N1**

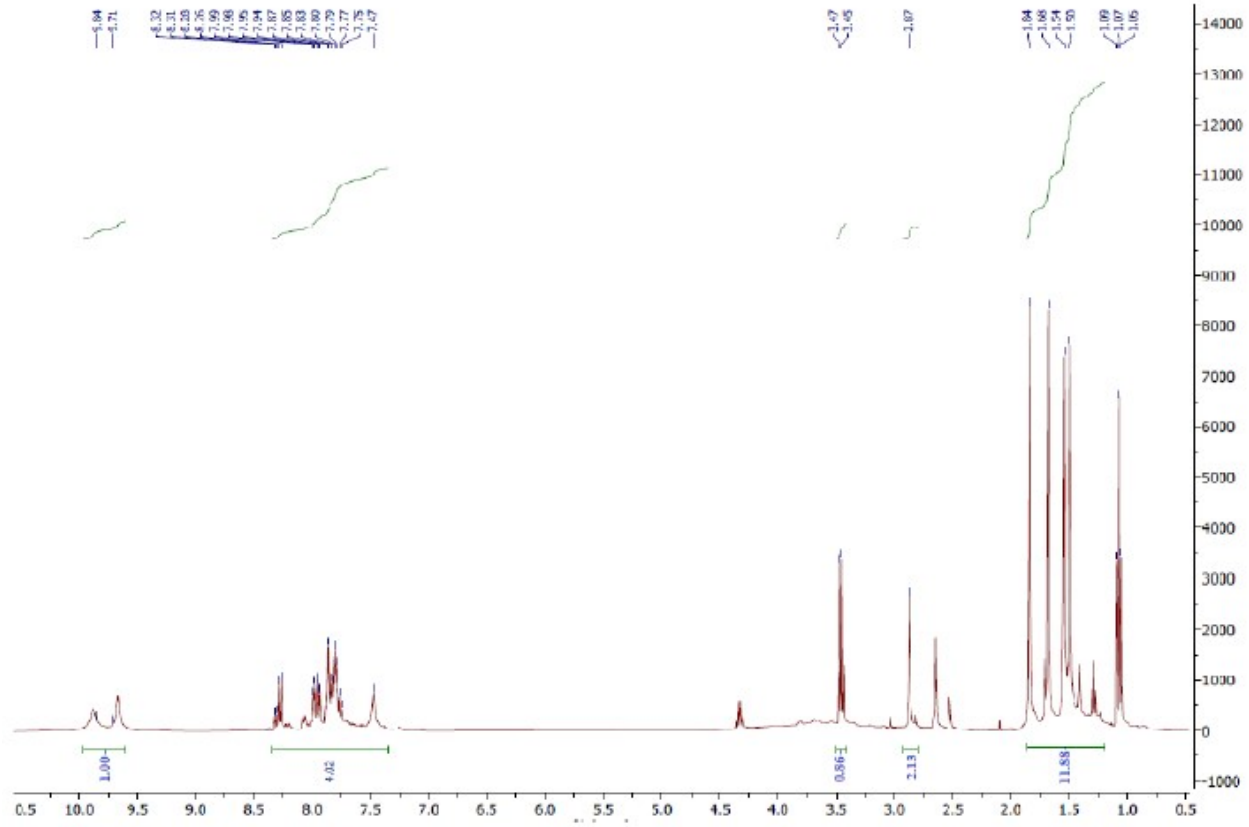

Fig. S4c. The recorded *[1]H NMR* spectrum of the compound **N1**

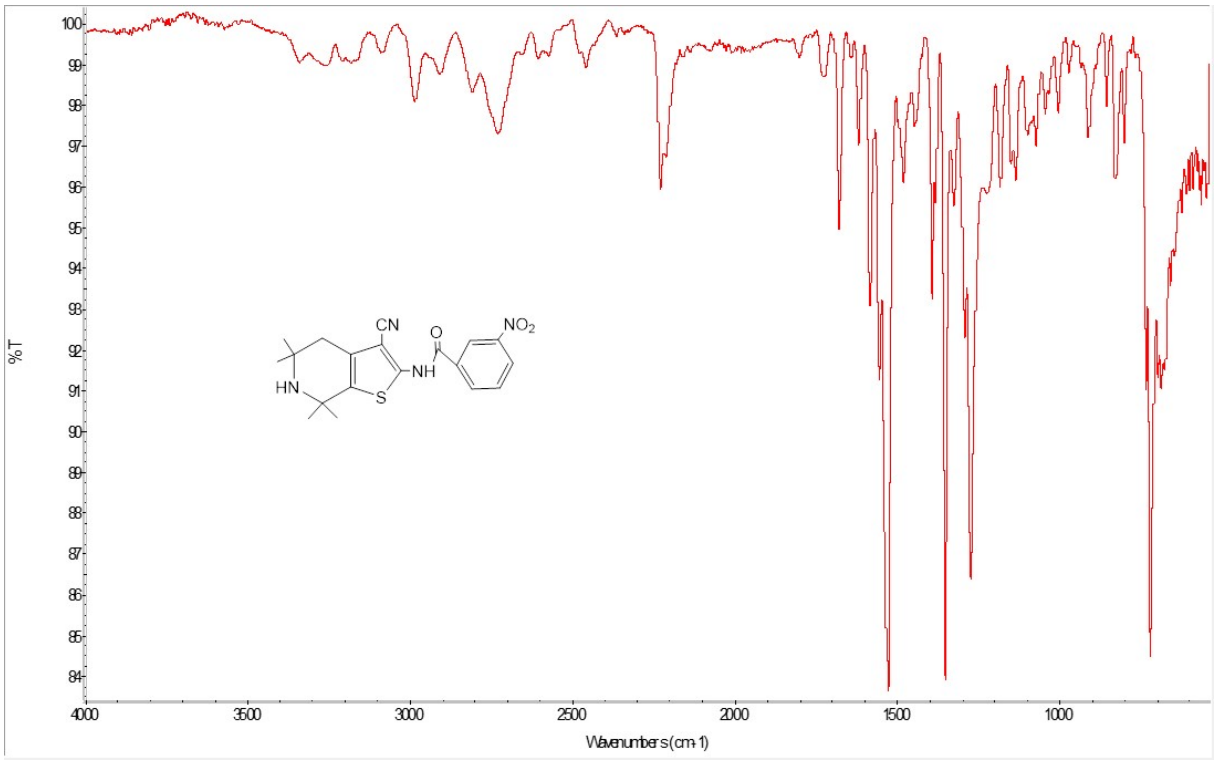

Fig. S5a. The recorded *FT-IR* spectrum of the compound **N2**

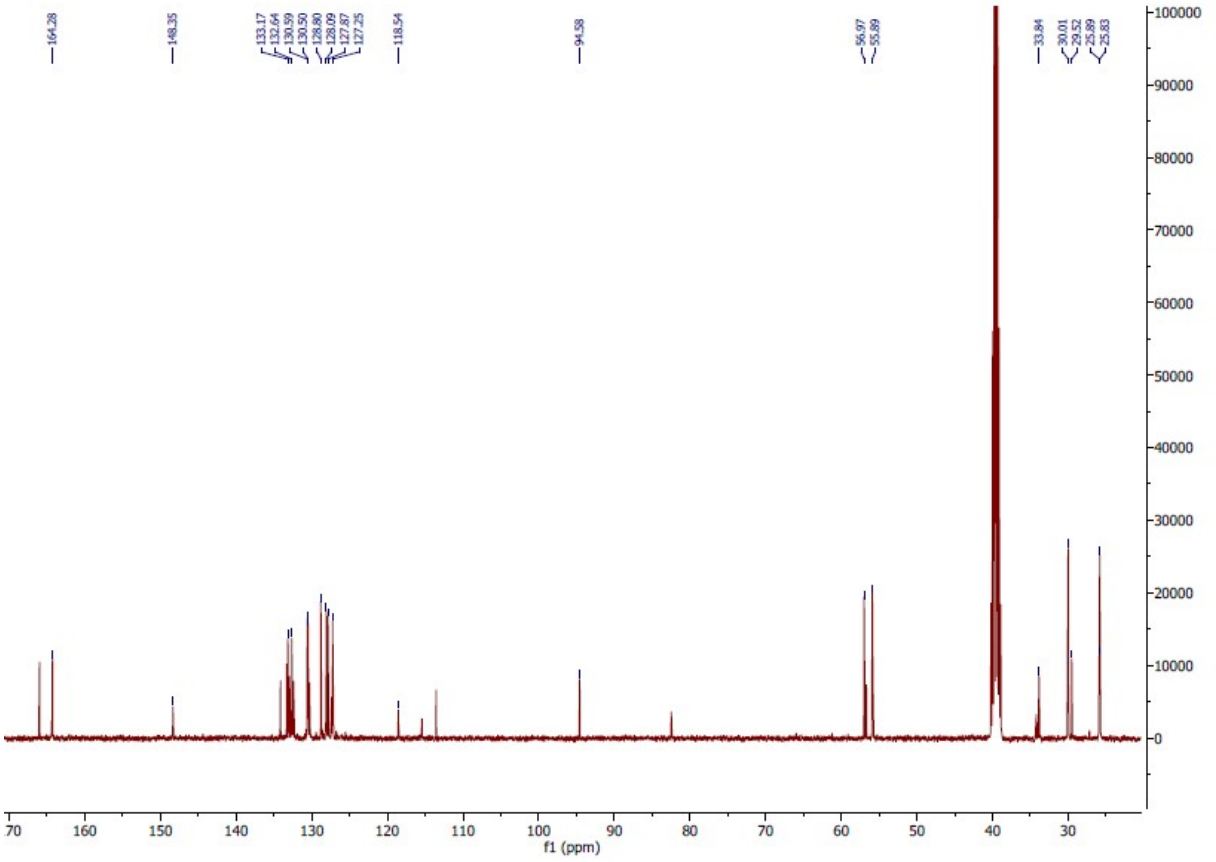

Fig. S5b. The recorded *^{13}C NMR* spectrum of the compound **N2**

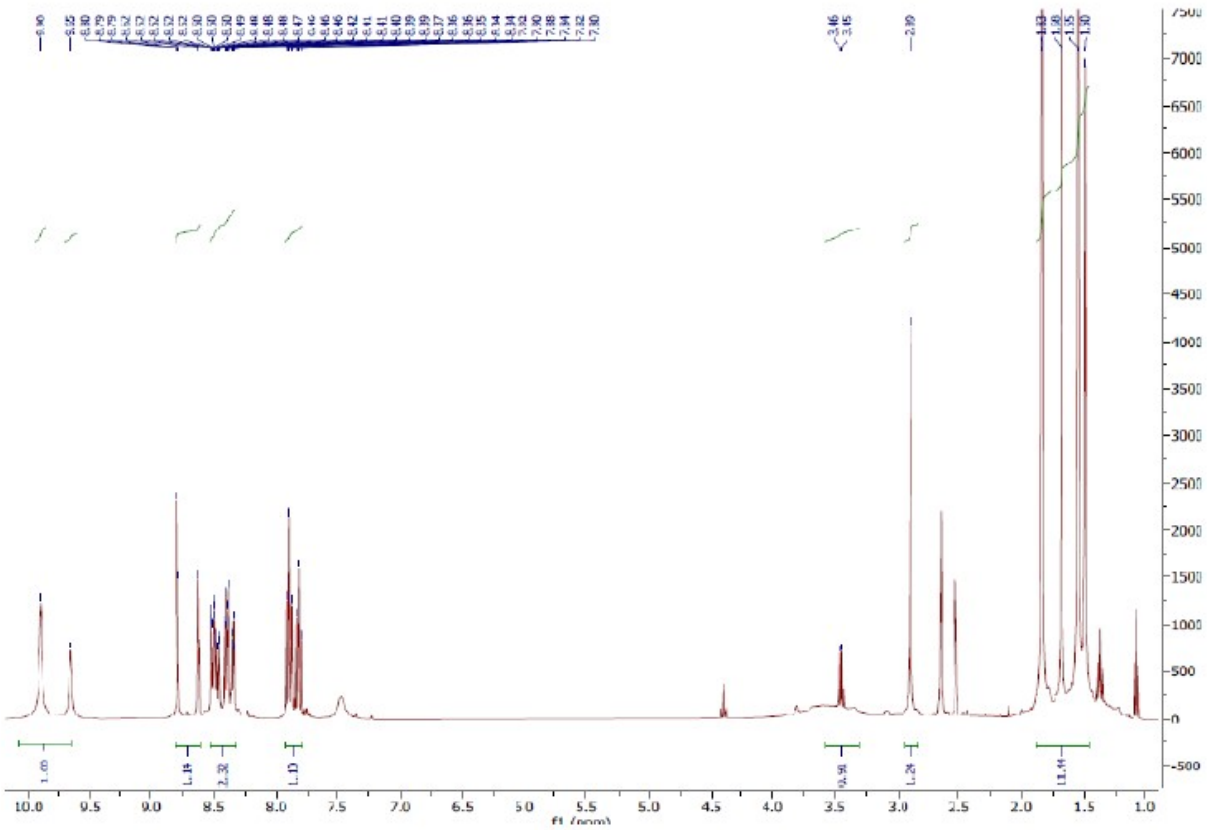

Fig. S5c. The recorded *^{1}H NMR* spectrum of the compound **N2**

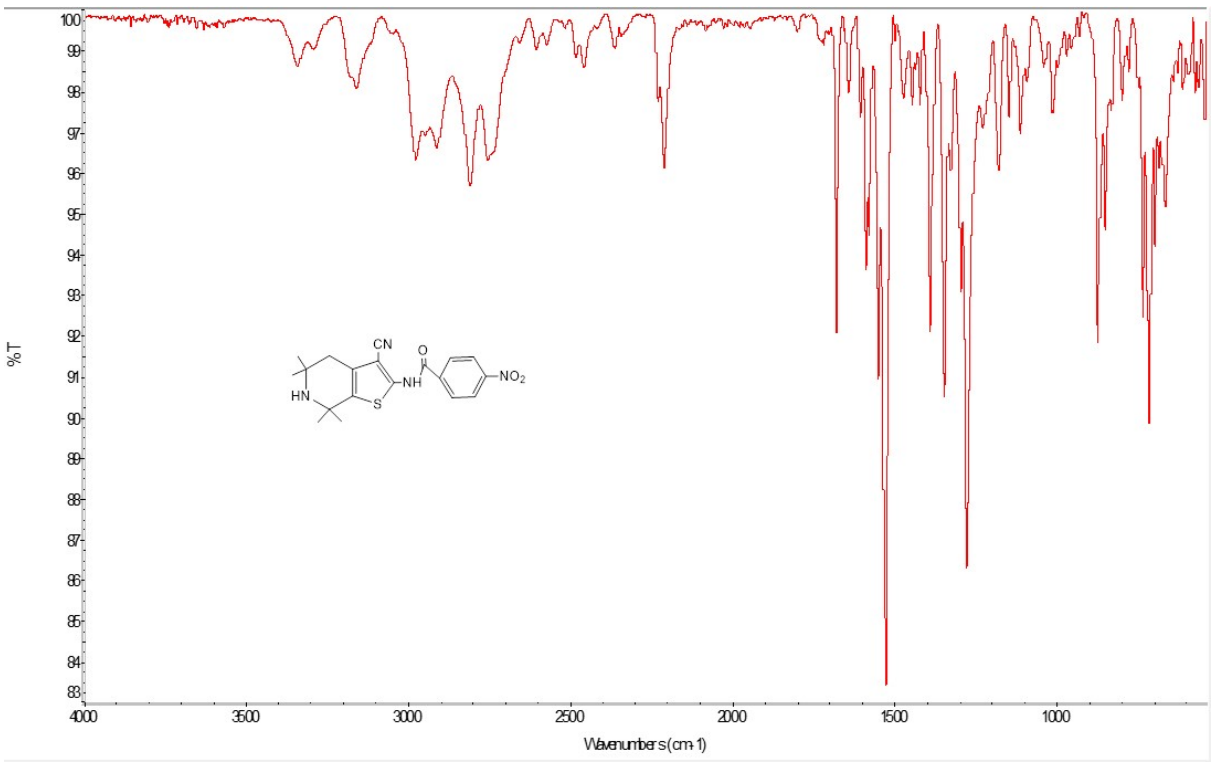

Fig. S6a. The recorded *FT-IR* spectrum of the compound **N3**

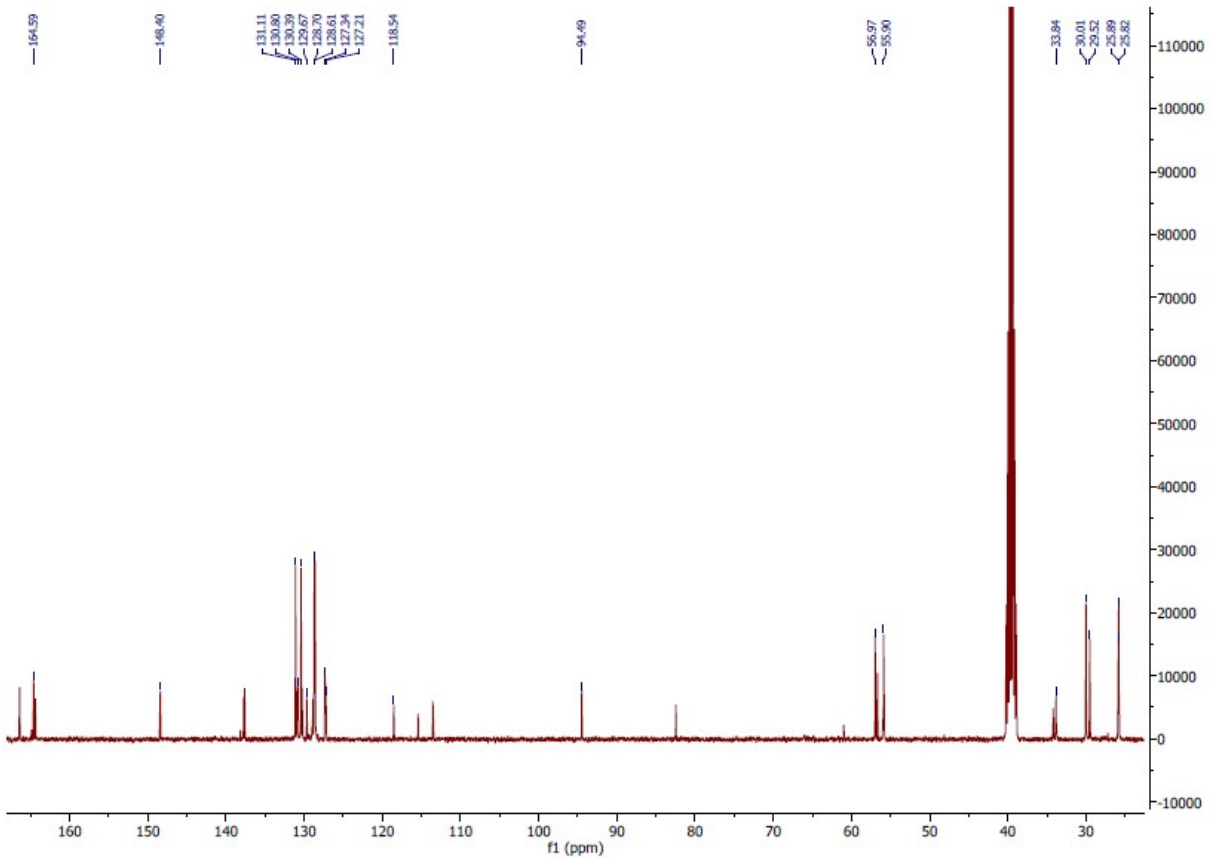

Fig. S6b. The recorded *[13]C NMR* spectrum of the compound **N3**

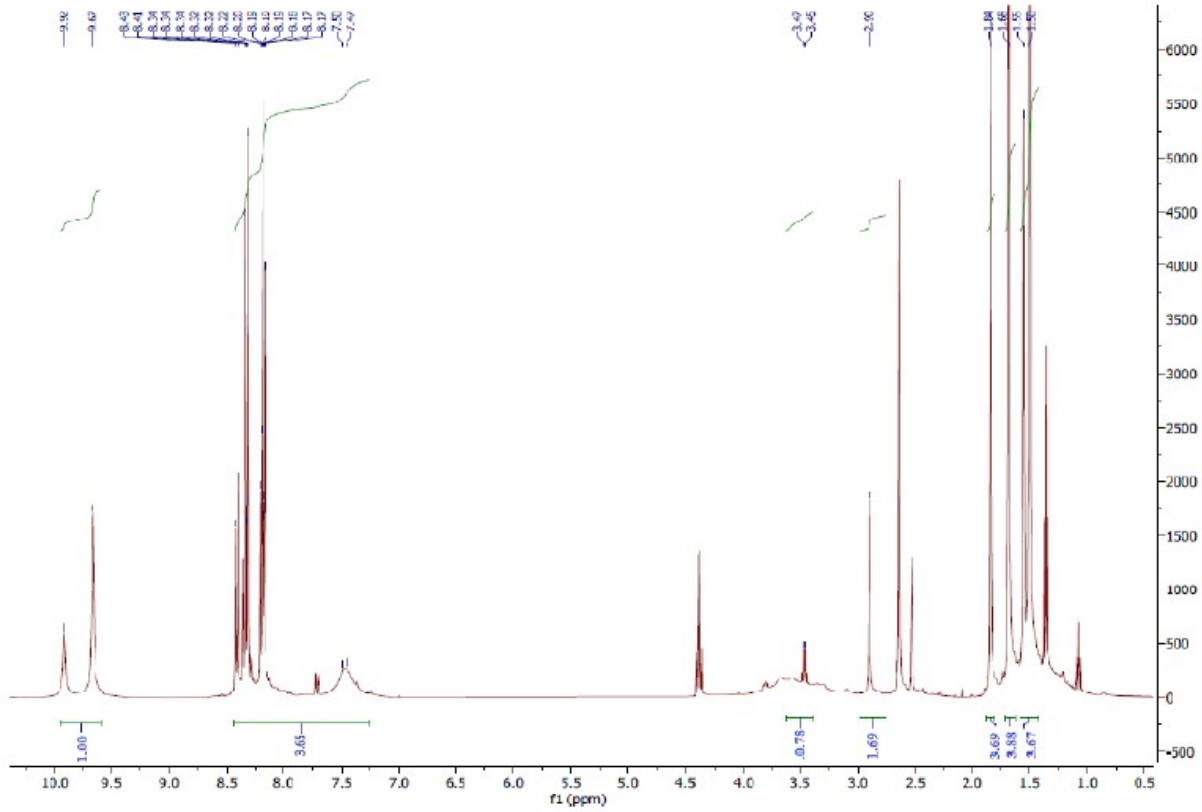

Fig. S6c. The recorded *[1]H NMR* spectrum of the compound **N3**

Table S1. The observed and calculated *^{13}C* NMR chemical shifts of compounds **1-6** relative to TMS, at B3LYP/6-311G** level of the theory in DMSO

	C1		***C2***		***C3***		***N1***		***N2***		***N3***	
Atom	***Exp.***	***Calc.***	***Exp.***	***Calc.***	***Exp.***	***Calc.***	***Exp.***	***Calc.***	***Exp.***	***Calc.***	***Exp.***	***Calc.***
1-C	56.9	60.2	56.9	60.1	56.9	60.1	56.0	60.2	56.9	60.2	56.6	60.2
2-C	33.8	41.7	33.8	41.7	33.8	41.8	34.2	41.8	33.8	41.7	34.2	41.8
3-C	55.9	57.4	55.8	57.4	55.9	57.4	55.9	57.4	55.9	57.4	55.8	57.4
6-C	93.4	97.4	94.5	97.2	94.6	97.0	93.1	97.6	94.8	97.7	94.8	98.0
7-C	147.9	161.5	148.3	161.7	148.4	161.8	145.8	161.2	147.5	161.5	150.0	161.3
9-C	134.2	148.9	132.6	149.0	130.8	148.7	133.0	149.3	134.9	149.5	130.6	149.7
10-C	130.2	138.5	130.5	138.5	130.3	138.5	127.3	138.6	127.5	138.7	130.0	138.9
13-C	164.8	169.6	164.2	167.9	164.5	168.1	164.3	170.0	163.6	167.3	165.7	167.6
15-C	131.9	140.6	130.5	140.5	128.7	137.2	129.8	140.0	130.5	140.4	130.5	145.5
16-C	127.1	135.9	127.8	130.3	127.2	133.2	124.2	135.2	130.2	139.3	127.2	132.9
17-C	132.5	147.6	128.0	136.5	129.6	138.4	134.5	156.3	123.2	131.8	127.5	138.0
18-C	130.5	134.6	128.8	137.4	127.3	135.9	132.3	143.4	127.2	137.2	123.5	131.2
20-C	129.6	138.3	133.1	150.4	128.6	136.7	123.6	133.1	135.3	157.1	123.6	131.3
21-C	130.7	140.0	132.6	140.6	131.1	154.7	127.2	138.6	123.6	134.7	136.4	158.5
23-C	118.5	119.9	118.5	120.1	118.5	120.1	118.5	119.8	113.5	120.0	118.5	119.9
24-C	---	---	---	---	---	---	---	---	---	---	---	---
25-C	---	---	---	---	---	---	---	---	---	---	---	---
27-C	29.5	34.5	25.9	34.5	25.9	34.5	25.9	34.5	29.5	34.5	29.5	34.5
28-C	---	---	---	---	---	---	---	---	---	---	---	---
29-C	---	---	---	---	---	---		---	---	---	---	---
31-C	25.8	29.5	25.8	29.5	25.8	29.4	25.8	29.5	25.9	29.5	25.8	29.4
32-C	---	---	---	---	---	---	---	---	---	---	---	---
33-C	---	---	---	---	---	---		---	---	---	---	---
35-C	25.9	35.2	29.5	35.2	29.5	35.2	29.5	35.2	25.8	25.2	25.9	35.2
36-C	---	---	---	---	---	---	---	---	---	---	---	---
37-C	---	---	---	---	---	---		---	---	---	---	---
39-C	29.9	37.2	30.0	37.2	30.0	37.1	29.9	37.1	30.0	37.2	30.0	37.2
40-C	---	---	---	---	---	---	---	---	---	---	---	---
41-C	---	---	---	---	---	---	---	---	---	---	---	---

Table S2. The observed and calculated *^{1}H* NMR chemical shifts of compounds **1-6** relative to TMS, at B3LYP/6-311G** level of the theory in DMSO

	C1		***C2***		***C3***		***N1***		***N2***		***N3***	
Atom	***Exp.***	***Calc.***	***Exp.***	***Calc.***	***Exp.***	***Calc.***	***Exp.***	***Calc.***	***Exp.***	***Calc.***	***Exp.***	***Calc.***
4-H	2.86	2.34	2.88	2.34	2.88	2.34	2.87	2.35	2.89	2.36	2.90	2.36
5-H	3.46	2.67	3.45	2.67	3.45	2.67	3.47	2.69	3.47	2.69	3.57	2.70
12-H	9.86	8.27	9.98	8.81	9.88	8.77	8.31	8.35	8.79	8.89	9.92	8.88
19-H	7.58	7.77	7.76	7.84	7.67	7.89	7.77	7.81	8.34	8.33	7.49	8.11
22-H	7.46	7.69	7.65	7.78	7.57	7.70	8.31	8.15	7.92	8.04	8.32	8.67
23-H	---	---	---	---	---	---	9.84	8.44	8.62	8.75	---	---
24-H	---	---	---	---	---	---	7.98	8.01	---	---	---	---
26-H	1.48	0.86	1.49	0.86	1.49	0.86	---	---	---	---	1.07	0.88
27-H	---	---	---	---	---	---	---	---	1.50	0.88	---	---
28-H	1.67	1.31	1.82	1.31	1.67	1.31	1.50	0.88	---	---	1.53	1.32
29-H	1.67	1.41	1.67	1.41	1.67	1.41	---	---	1.68	1.32	1.53	1.42
30-H	1.52	0.97	1.49	0.96	1.49	0.96	1.68	1.32	1.68	1.42	1.07	0.98
31-H	---	---	---	---	---	---	1.68	1.42	1.55	0.97	---	---
32-H	1.48	0.94	1.49	0.94	1.49	0.93	1.50	0.97	---	---		0.94
33-H	1.48	0.96	1.54	0.96	1.53	0.95	---	---	1.50	0.95	1.36	0.96
34-H	1.82	1.47	1.67	1.47	1.83	1.46	1.50	0.96	1.50	0.97	1.72	1.46
35-H	---	---	---	---	---	---	1.54	0.98	1.83	1.48	---	---
36-H	1.67	1.33	1.67	1.32	1.67	1.32	1.84	1.50	---	---	1.53	1.33
37-H	1.52	1.29	1.54	1.28	1.53	1.28	---	---	1.68	1.34	1.36	1.29
38-H	2.63	1.80	2.64	1.79	2.63	1.78	1.68	1.32	1.55	1.30	2.60	1.80

39-H	---	---	---	---	---	---	1.54	1.29	2.65	1.81	---	---
40-H	1.52	1.10	1.54	1.09	1.53	1.09	2.64	1.81	---	---	1.36	1.11
41-H	1.82	1.55	1.82	1.54	1.82	1.54	---	---	1.55	1.11	1.72	1.56
42-H	1.82	1.46	1.82	1.46	1.82	1.45	1.54	1.11	1.83	1.56	1.72	1.47
43-H	7.64	7.80	7.92	8.27	8.0	8.36	1.84	1.55	1.83	1.47	8.18	8.56
44-H	7.51	7.71	7.74	7.79	7.95	7.74	1.84	1.46	9.90	9.23	8.34	8.68

Table S3. The theoretical UV-Vis absorption characteristics of the studied compounds, in methanol.

Exp. (λnm)	Transitions	MO%	*ΔE (eV)*	*λ (nm)*	*f*
	C1				
300	H→L	(98%)	3.7921	327	0.3830
	H-1→L	(97%)	4.0171	309	0.0010
	H-3→L H-2→L H→L+1	(7.3%) (11.2%) (77.8%)	4.6074	269	0.0404
	H-3→L H→L+2	(17.5%) (75.4%)	4.6436	267	0.0019
257	H-5→L H-4→L H-3→L H→L+1 H→L+2	(18%) (16.2%) (41%) (6.4%) (13%)	4.7091	263	0.0202
	H-5→L H-4→L H-3→L H→L+2	(20.4%) (37.9%) (21.7%) (9.2%)	4.7563	261	0.0126
	C2				
311	H→L	(99%)	3.5756	347	0.4155
	H-1→L	(98%)	3.8563	322	0.0011
	H-3→L H-2→L H→L+1	(25.6%) (9.3%) (57%)	4.5125	275	0.0291
	H-5→L H-4→L H-3→L H-2→L H→L+2	(7.6%) (10%) (17.5%) (45.6%) (11.3%)	4.5551	272	0.0177
	H-5→L H-4→L H-2→L H→L+1	(44%) (27.1%) (17.2%) (4.2%)	4.6096	269	0.0228
	H-5→L H-3→L H-2→L H→L+1	(7.5%) (31.6%) (20%) (33.8%)	4.6706	266	0.0725
	C3				
306	H→ L	(99%)	3.5809	346	0.4577
	H-1→L	(98%)	3.8833	319	0.0012
238	H-2→L H→L+1	(13.7%) (82.5%)	4.5126	275	0.0501
	H-5→L H-4→L H-3→L H-2→L H→L+2	(35.3%) (9.2%) (15.6%) (16.2%) (16.9%)	4.5716	271	0.0425
	H-5→L H-4→L	(21.4%) (14.4%)	4.6154	269	0.0321

	H-2→L H→L+1 H→L+2	(45.4%) (6.3%) (9.2%)			
	H-5→L H-2→L H→L+2	(12%) (16.6%) (61.2%)	4.7023	264	0.0475
	N1				
	H→L	(99.6%)	2.7380	453	0.0067
	H-1→L	(99.8%)	3.1828	390	0.0002
	H-2→L	(97.8%)	3.8203	325	0.0266
	H-6→L H-4→L H-3→L	(48.9%) (30.2%) (11.2%)	3.8463	322	0.0266
296	H-3→L H→L+1	(20.1%) (69.7%)	3.9794	312	0.3421
	H-3→L H→L+1	(62.6%) (26.2%)	4.0489	306	0.0315
	N2				
	H→L	(99.7%)	2.8280	438	0.0025
	H-1→L	(99.8%)	3.2213	385	0.0003
	H→L+1	(98.8%)	3.5553	349	0.4221
	H+1→L+1	(97.7%)	3.8054	326	0.0009
	H-6→L	(93.7%)	3.8679	321	0.0000
	H-2→L	(99.2%)	3.9000	318	0.0017
	N3				
	H→L	(99.7%)	2.6896	461	0.1714
	H-1→L	(99.4%)	3.0181	411	0.0013
	H-2→L	(98.7%)	3.7126	334	0.0184
	H-6→L H-6→L+1	(89.8%) (5.6%)	3.7992	326	0.0007
304	H-3→L H→L+1	(16.6%) (77.5%)	3.9959	310	0.3686
	H-5→L H-3→L H→L+1	(9%) (66.1%) (16.6%)	4.0647	305	0.0069

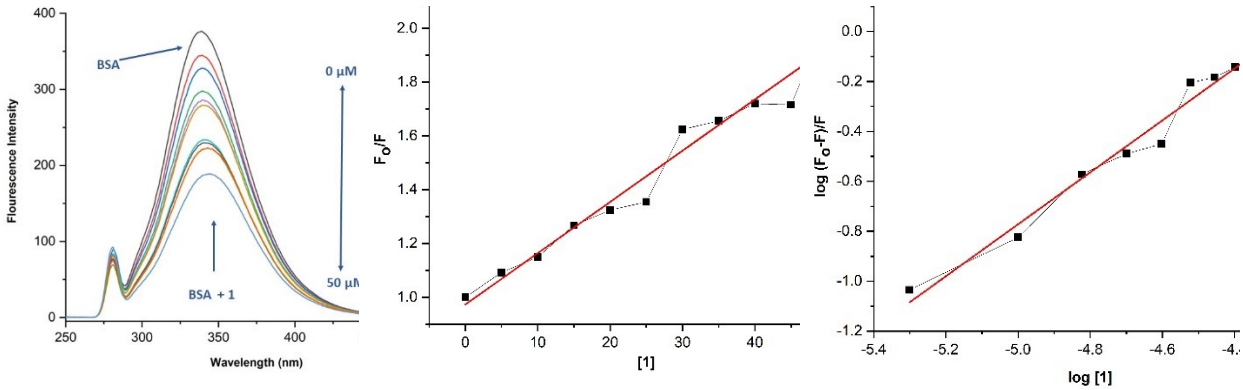

(a) **(b)** **(c)**

Fig. S7. (a) The fluorescence spectra of BSA with presence of **C1**, **(b)** Stern-Volmer plot of **C1** to BSA at 293 K, **(c)** The plot of $\log(F_0 - F)/F$ vs. log[**C1**] for quenching of **C1** to BSA (λex = 280 nm; λem = 338 nm. [BSA] = 1.00×10^{-5} mol L^{-1}, [**C1**] : 0, 5, 10, 15, 20, 25, 30, 35, 40, 45, 50 ($\times 10^{-6}$ mol L^{-1})

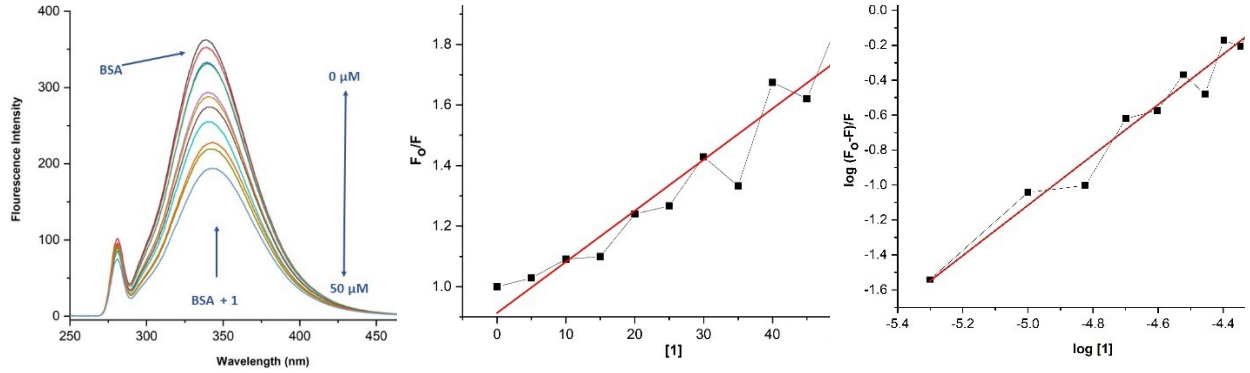

(a) **(b)** **(c)**

Fig. S8. (a) The fluorescence spectra of BSA with presence of **C1**, **(b)** Stern-Volmer plot of **C1** to BSA at 298 K , **(c)** The plot of log(F_0 −F)/F vs. log[**C1**] for quenching of **C1** to BSA (λex = 280 nm; λem = 338 nm. [BSA] = 1.00x10^{-5} mol L^{-1}, [**C1**] : 0, 5, 10, 15, 20, 25, 30, 35, 40, 45, 50 (x10^{-6} mol L^{-1})

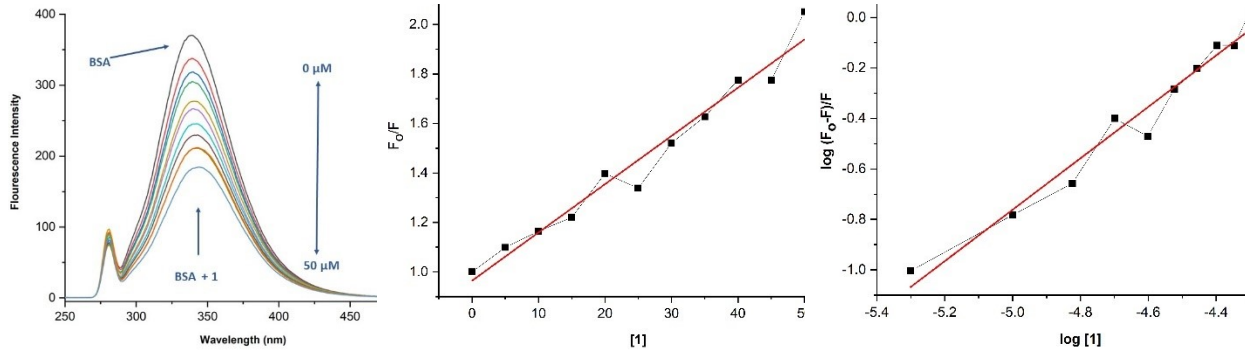

(a) **(b)** **(c)**

Fig. S9. (a) The fluorescence spectra of BSA with presence of **C1**, **(b)** Stern-Volmer plot of **C1** to BSA at 308 K, **(c)** The plot of log(F_0 −F)/F vs. log[**C1**] for quenching of **C1** to BSA (λex = 280 nm; λem = 338 nm. [BSA] = 1.00x10^{-5} mol L^{-1}, [**C1**] : 0, 5, 10, 15, 20, 25, 30, 35, 40, 45, 50 (x10^{-6} mol L^{-1})

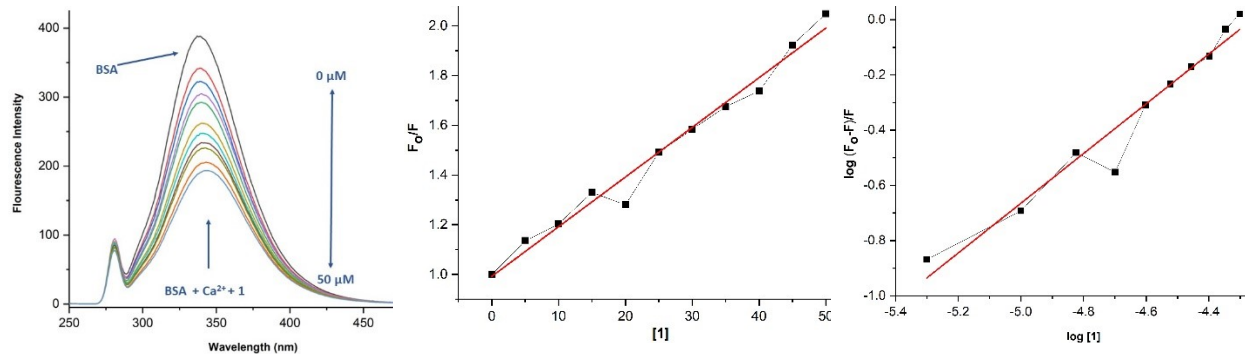

(a) **(b)** **(c)**

Fig. S10. (a) The fluorescence spectra of BSA with presence of **C1** and **Ca^{2+}** (1.00x10^{-5} mol L^{-1}), **(b)** Stern-Volmer plot of **C1** to BSA at 298 K with presence **Ca^{2+}**, **(c)** The plot of log(F_0 −F)/F vs. log[**C1**] for quenching of **C1** to BSA with presence **Ca^{2+}** (1.00x10^{-5} mol L^{-1}) (λex = 280 nm; λem = 338 nm. [BSA] = 1.00x10^{-5} mol L^{-1}, [**C1**] : 0, 5, 10, 15, 20, 25, 30, 35, 40, 45, 50 (x10^{-6} mol L^{-1})

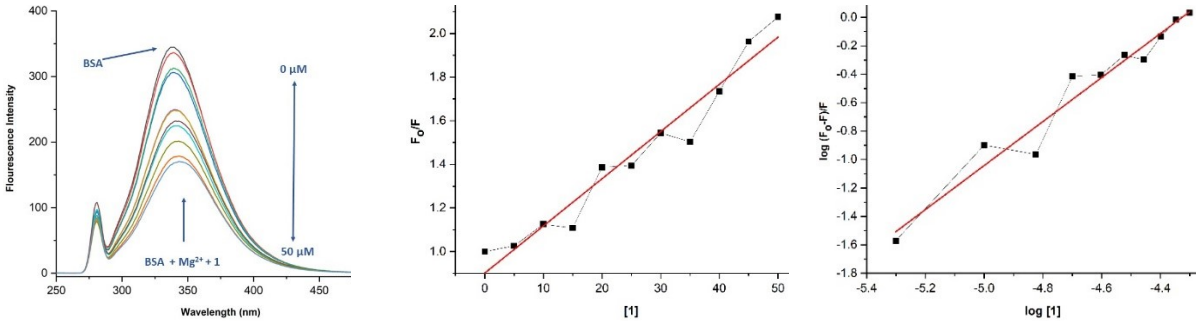

(a) **(b)** **(c)**

Fig. S11. (a) The fluorescence spectra of BSA with presence of **C1** and Mg^{2+} ($1.00x10^{-5}$ mol L^{-1}), **(b)** Stern-Volmer plot of **C1** to BSA at 298 K with presence Mg^{2+}, **(c)** The plot of $\log(F_0 - F)/F$ vs. log[**C1**] for quenching of **C1** to BSA with presence Mg^{2+} ($1.00x10^{-5}$ mol L^{-1}) (λex = 280 nm; λem = 338 nm. [BSA] = $1.00x10^{-5}$ mol L^{-1}, [**C1**] : 0, 5, 10, 15, 20, 25, 30, 35, 40, 45, 50 ($x10^{-6}$ mol L^{-1})

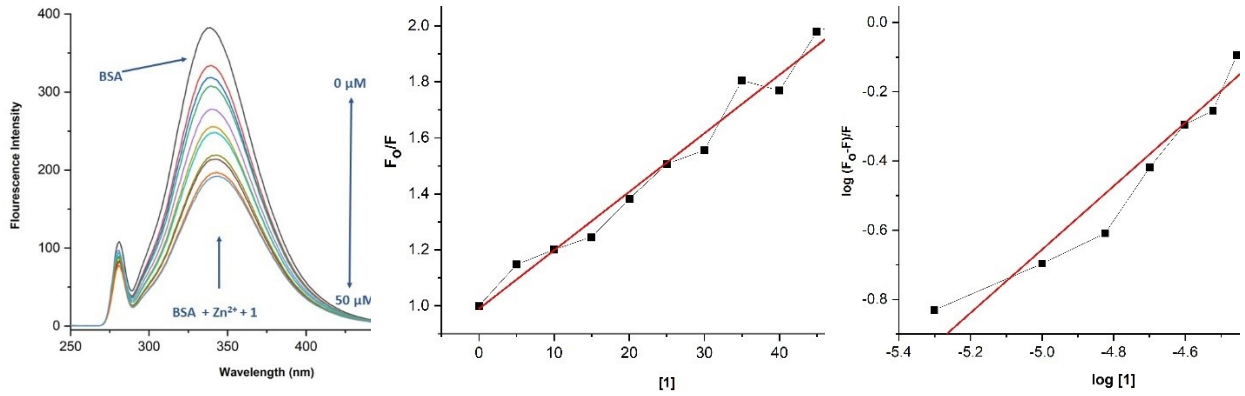

(a) **(b)** **(c)**

Fig. S12. (a) The fluorescence spectra of BSA with presence of **C1** and Zn^{2+} ($1.00x10^{-5}$ mol L^{-1}), **(b)** Stern-Volmer plot of **C1** to BSA at 298 K with presence Zn^{2+}, **(c)** The plot of $\log(F_0 - F)/F$ vs. log[**C1**] for quenching of **C1** to BSA with presence Zn^{2+} ($1.00x10^{-5}$ mol L^{-1}) (λex = 280 nm; λem = 338 nm. [BSA] = $1.00x10^{-5}$ mol L^{-1}, [**C1**] : 0, 5, 10, 15, 20, 25, 30, 35, 40, 45, 50 ($x10^{-6}$ mol L^{-1})

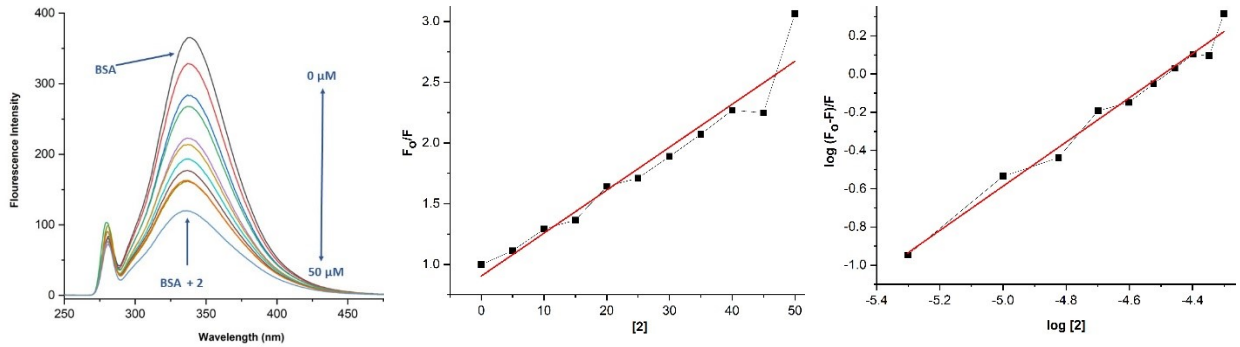

(a) **(b)** **(c)**

Fig. S13. (a) The fluorescence spectra of BSA with presence of **C2**, **(b)** Stern-Volmer plot of **C2** to BSA at 293 K , **(c)** The plot of $\log(F_0 - F)/F$ vs. log[**C2**] for quenching of **C2** to BSA (λex = 280 nm; λem = 338 nm. [BSA] = $1.00x10^{-5}$ mol L^{-1}, [**C2**] : 0, 5, 10, 15, 20, 25, 30, 35, 40, 45, 50 ($x10^{-6}$ mol L^{-1})

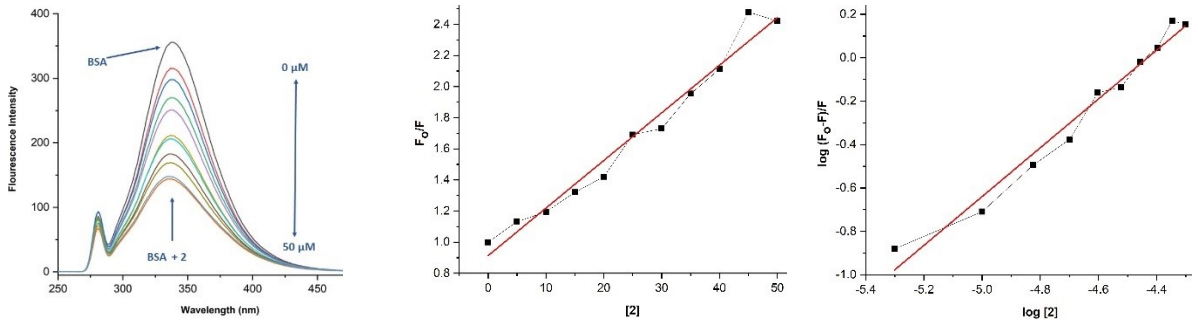

(a) **(b)** **(c)**

Fig. S14. (a) The fluorescence spectra of BSA with presence of **C2**, **(b)** Stern-Volmer plot of **C2** to BSA at 308 K , **(c)** The plot of log(F_0 −F)/F vs. log[**C2**] for quenching of **C2** to BSA (λex = 280 nm; λem = 338 nm. [BSA] = 1.00x10^{-5} mol L^{-1}, [**C2**] : 0, 5, 10, 15, 20, 25, 30, 35, 40, 45, 50 (x10^{-6} mol L^{-1})

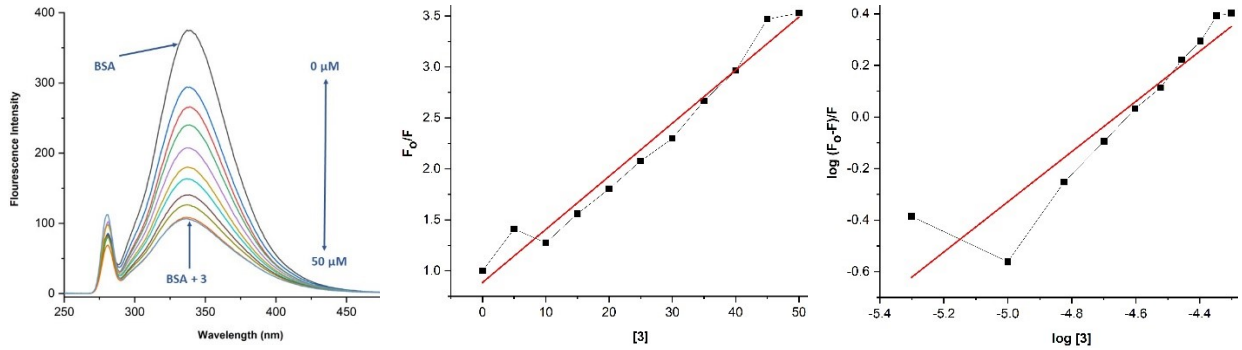

(a) **(b)** **(c)**

Fig. S15. (a) The fluorescence spectra of BSA with presence of **C3**, **(b)** Stern-Volmer plot of **C3** to BSA at 293 K, **(c)** The plot of log(F_0 −F)/F vs. log[**C3**] for quenching of **C3** to BSA (λex = 280 nm; λem = 338 nm. [BSA] = 1.00x10^{-5} mol L^{-1}, [**C3**] : 0, 5, 10, 15, 20, 25, 30, 35, 40, 45, 50 (x10^{-6} mol L^{-1})

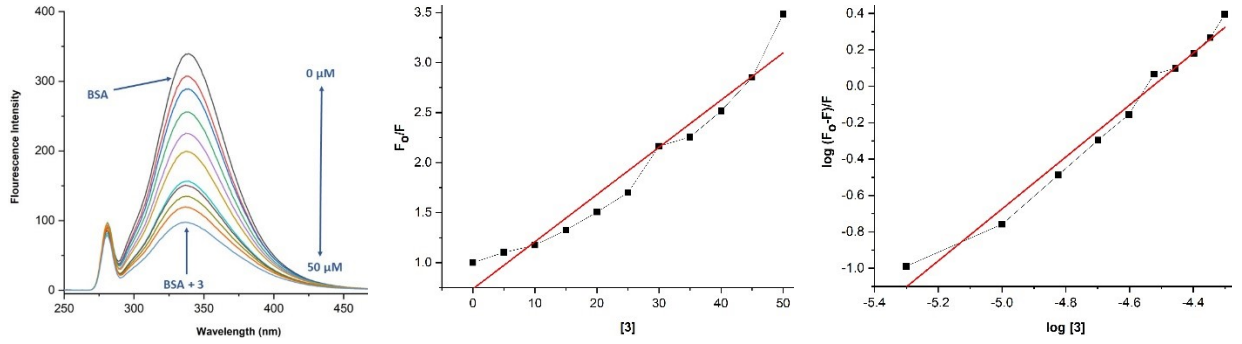

(a) **(b)** **(c)**

Fig. S16. (a) The fluorescence spectra of BSA with presence of **C3**, **(b)** Stern-Volmer plot of **C3** to BSA at 298 K , **(c)** The plot of log(F_0 −F)/F vs. log[**C3**] for quenching of **C3** to BSA (λex = 280 nm; λem = 338 nm. [BSA] = 1.00x10^{-5} mol L^{-1}, [**C3**] : 0, 5, 10, 15, 20, 25, 30, 35, 40, 45, 50 (x10^{-6} mol L^{-1})

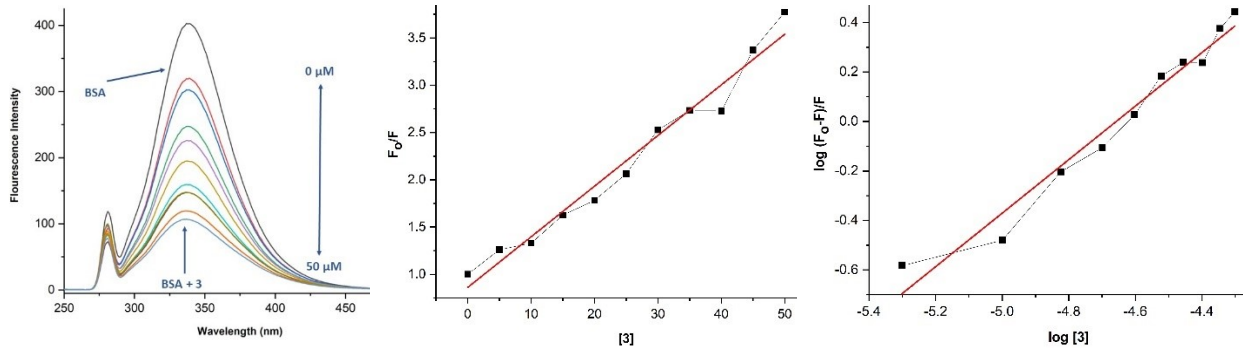

(a) **(b)** **(c)**

Fig. S17. (a) The fluorescence spectra of BSA with presence of **C3**, **(b)** Stern-Volmer plot of **C3** to BSA at 308 K **(c)** The plot of log(F_0 −F)/F vs. log[**C3**] for quenching of **C3** to BSA (λex = 280 nm; λem = 338 nm. [BSA] = 1.00x10^{-5} mol L^{-1}, [**C3**] : 0, 5, 10, 15, 20, 25, 30, 35, 40, 45, 50 (x10^{-6} mol L^{-1})

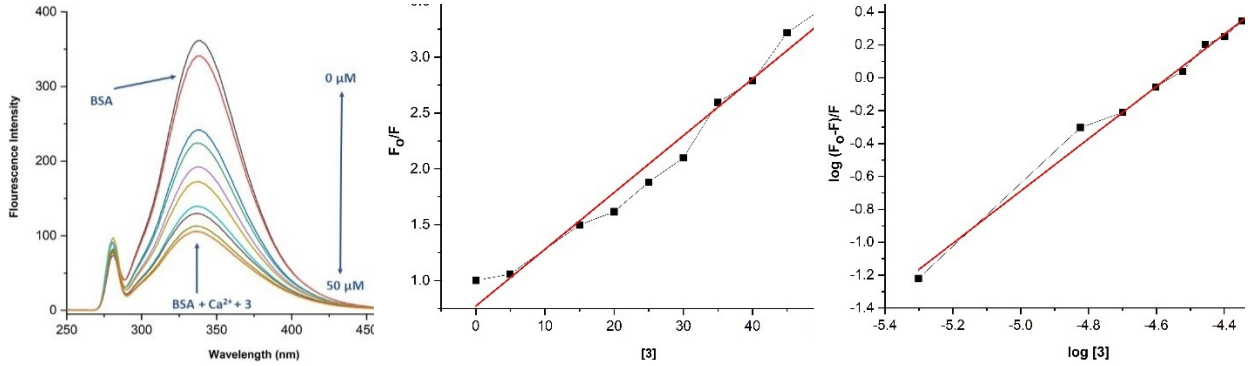

(a) **(b)** **(c)**

Fig. S18. (a) The fluorescence spectra of BSA with presence of **C3** and **Ca^{2+}** (1.00x10^{-5} mol L^{-1}), **(b)** Stern-Volmer plot of **C3** to BSA at 298 K with presence **Ca^{2+}**, **(c)** The plot of log(F_0 −F)/F vs. log[**C3**] for quenching of **C3** to BSA with presence **Ca^{2+}** (1.00x10^{-5} mol L^{-1}) (λex = 280 nm; λem = 338 nm. [BSA] = 1.00x10^{-5} mol L^{-1}, [**C3**] : 0, 5, 10, 15, 20, 25, 30, 35, 40, 45, 50 (x10^{-6} mol L^{-1})

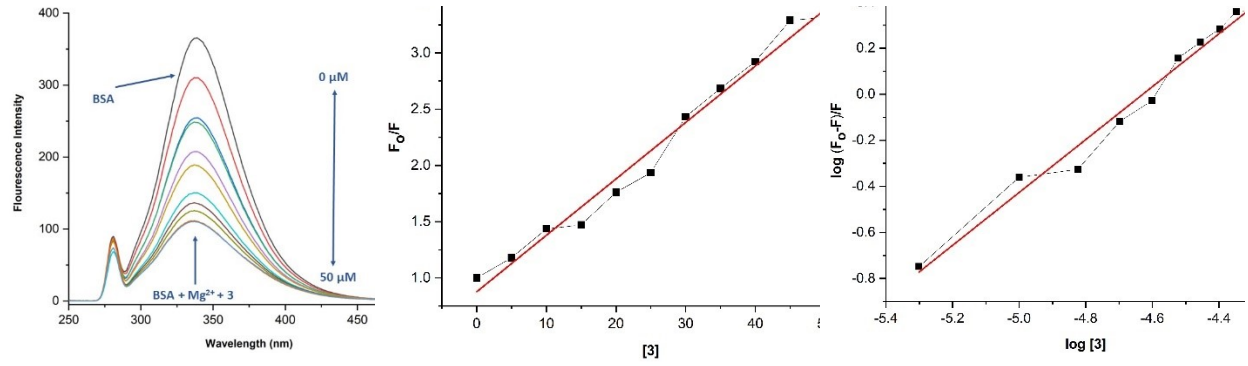

(a) **(b)** **(c)**

Fig. S19. (a) The fluorescence spectra of BSA with presence of **C3** and **Mg^{2+}** (1.00x10^{-5} mol L^{-1}), **(b)** Stern-Volmer plot of **C3** to BSA at 298 K with presence **Mg^{2+}**, **(c)** The plot of log(F_0 −F)/F vs. log[**C3**] for quenching of **C3** to BSA with presence **Mg^{2+}** (1.00x10^{-5} mol L^{-1}) (λex = 280 nm; λem = 338 nm. [BSA] = 1.00x10^{-5} mol L^{-1}, [**C3**] : 0, 5, 10, 15, 20, 25, 30, 35, 40, 45, 50 (x10^{-6} mol L^{-1})

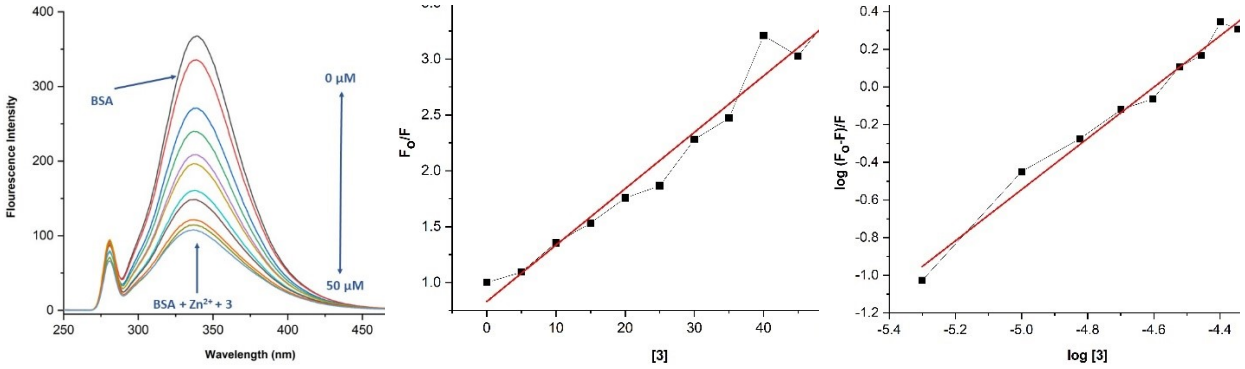

(a) **(b)** **(c)**

Fig. S20. (a) The fluorescence spectra of BSA with presence of **C3** and Zn^{2+} ($1.00x10^{-5}$ mol L^{-1}), **(b)** Stern-Volmer plot of **C3** to BSA at 298 K with presence Zn^{2+}, **(c)** The plot of $\log(F_0 - F)/F$ vs. log[**C3**] for quenching of **C3** to BSA with presence Zn^{2+} ($1.00x10^{-5}$ mol L^{-1}) (λex = 280 nm; λem = 338 nm. [BSA] = $1.00x10^{-5}$ mol L^{-1}, [**C3**] : 0, 5, 10, 15, 20, 25, 30, 35, 40, 45, 50 ($x10^{-6}$ mol L^{-1})

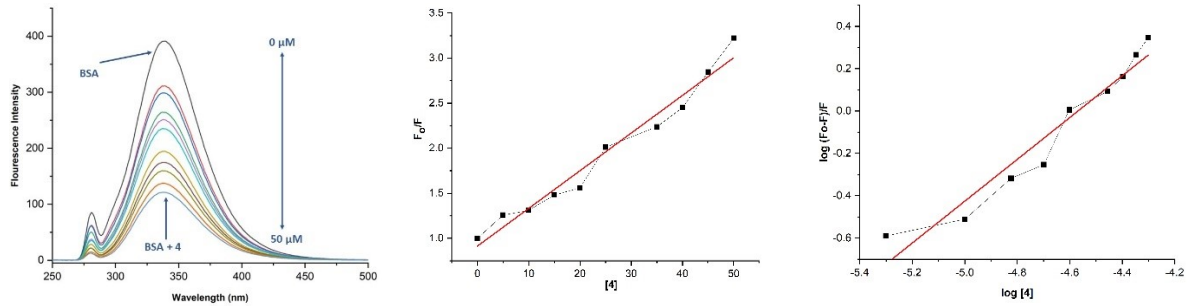

(a) **(b)** **(c)**

Fig. S21. (a) The fluorescence spectra of BSA with presence of **N1**, **(b)** Stern-Volmer plot of **N1** to BSA at 293 K, **(c)** The plot of $\log(F_0 - F)/F$ vs. log[**N1**] for quenching of **N1** to BSA (λex = 280 nm; λem = 338 nm. [BSA] = $1.00x10^{-5}$ mol L^{-1}, [**N1**] : 0, 5, 10, 15, 20, 25, 30, 35, 40, 45, 50 ($x10^{-6}$ mol L^{-1})

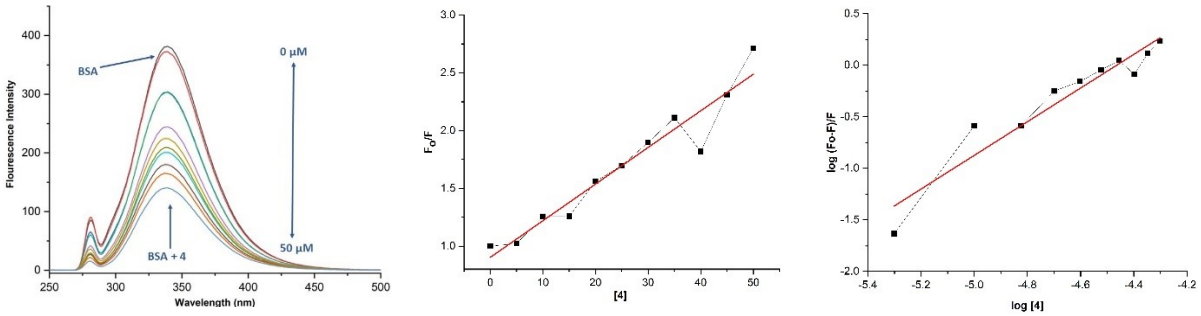

(a) **(b)** **(c)**

Fig. S22. (a) The fluorescence spectra of BSA with presence of **N1**, **(b)** Stern-Volmer plot of **N1** to BSA at 298 K, **(c)** The plot of $\log(F_0 - F)/F$ vs. log[**N1**] for quenching of **N1** to BSA (λex = 280 nm; λem = 338 nm. [BSA] = $1.00x10^{-5}$ mol L^{-1}, [**N1**] : 0, 5, 10, 15, 20, 25, 30, 35, 40, 45, 50 ($x10^{-6}$ mol L^{-1})

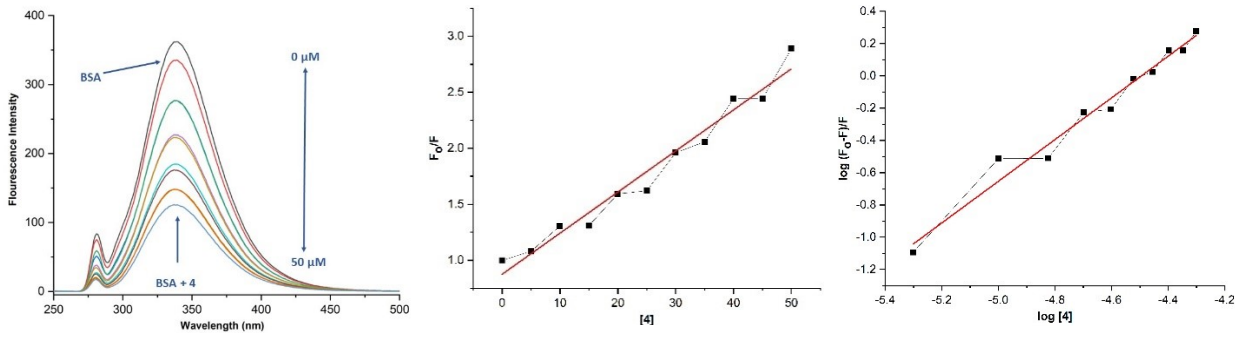

(a) **(b)** **(c)**

Fig. S23. (a) The fluorescence spectra of BSA with presence of **N1**, **(b)** Stern-Volmer plot of **N1** to BSA at 308 K, **(c)** The plot of log(F_0 −F)/F vs. log[**N1**] for quenching of **N1** to BSA (λex = 280 nm; λem = 338 nm. [BSA] = 1.00x10^{-5} mol L^{-1}, [**N1**] : 0, 5, 10, 15, 20, 25, 30, 35, 40, 45, 50 (x10^{-6} mol L^{-1})

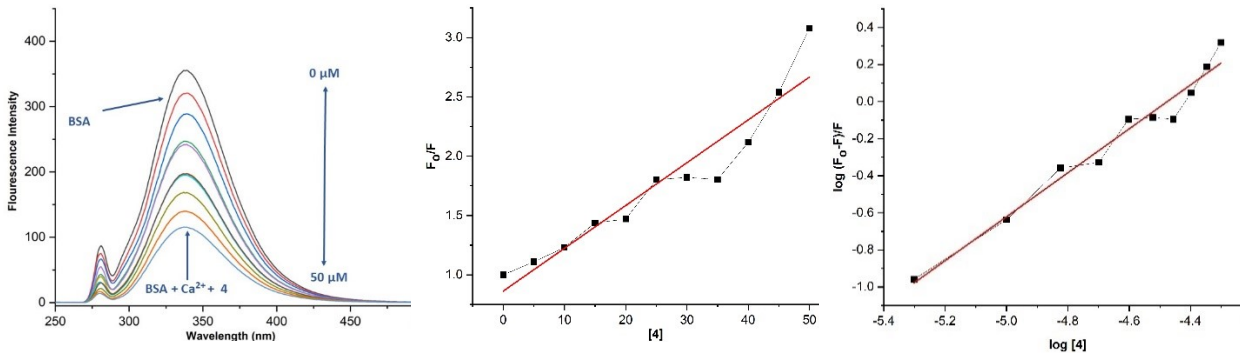

(a) **(b)** **(c)**

Fig. S24. (a) The fluorescence spectra of BSA with presence of **N1** and **Ca^{2+}** (1.00x10^{-5} mol L^{-1}), **(b)** Stern-Volmer plot of **N1** to BSA at 298 K with presence **Ca^{2+}**, **(c)** The plot of log(F_0 −F)/F vs. log[**N1**] for quenching of **N1** to BSA with presence **Ca^{2+}** (1.00x10^{-5} mol L^{-1}) (λex = 280 nm; λem = 338 nm. [BSA] = 1.00x10^{-5} mol L^{-1}, [**N1**] : 0, 5, 10, 15, 20, 25, 30, 35, 40, 45, 50 (x10^{-6} mol L^{-1})

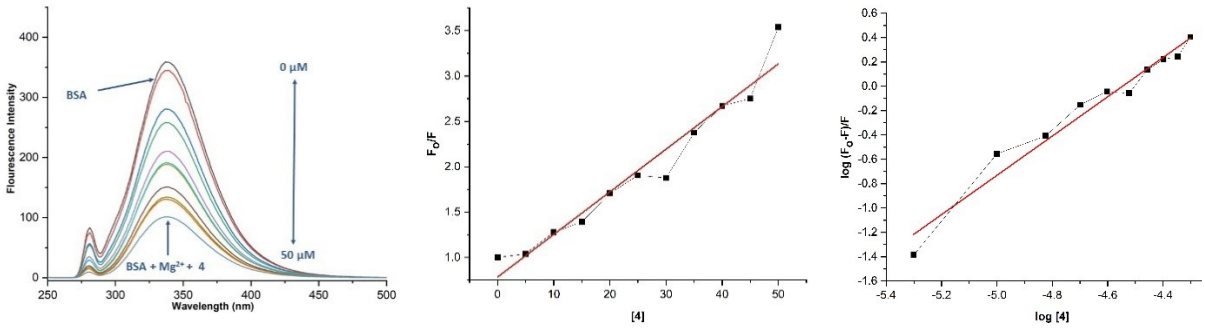

(a) **(b)** **(c)**

Fig. S25. (a) The fluorescence spectra of BSA with presence of **N1** and **Mg^{2+}** (1.00x10^{-5} mol L^{-1}), **(b)** Stern-Volmer plot of **N1** to BSA at 298 K with presence **Mg^{2+}**, **(c)** The plot of log(F_0 −F)/F vs. log[**N1**] for quenching of **N1** to BSA with presence **Mg^{2+}** (1.00x10^{-5} mol L^{-1}) (λex = 280 nm; λem = 338 nm. [BSA] = 1.00x10^{-5} mol L^{-1}, [**N1**] : 0, 5, 10, 15, 20, 25, 30, 35, 40, 45, 50 (x10^{-6} mol L^{-1})

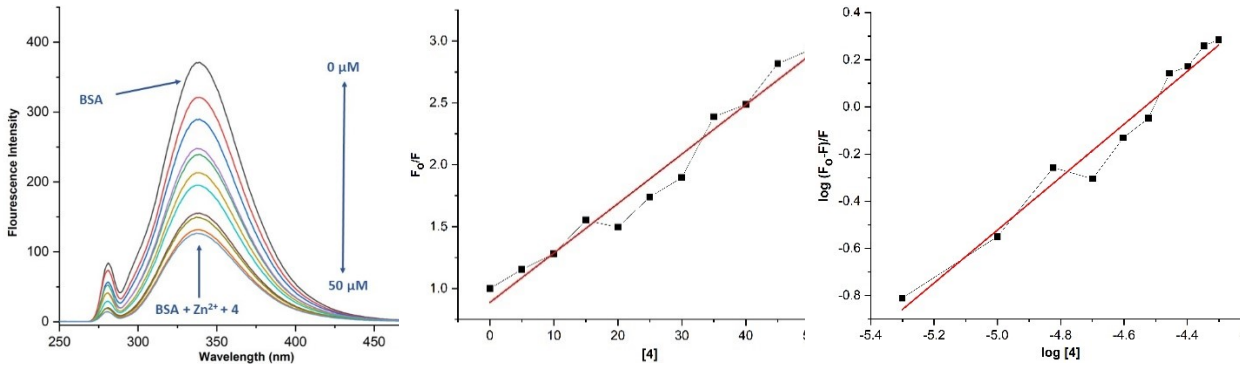

(a) **(b)** **(c)**

Fig. S26. (a) The fluorescence spectra of BSA with presence of **N1** and $\mathbf{Zn^{2+}}$ ($1.00x10^{-5}$ mol L^{-1}), **(b)** Stern-Volmer plot of **N1** to BSA at 298 K with presence $\mathbf{Zn^{2+}}$, **(c)** The plot of log(F_0 −F)/F vs. log[**N1**] for quenching of **N1** to BSA with presence $\mathbf{Zn^{2+}}$ ($1.00x10^{-5}$ mol L^{-1}) (λex = 280 nm; λem = 338 nm. [BSA] = $1.00x10^{-5}$ mol L^{-1}, [**N1**] : 0, 5, 10, 15, 20, 25, 30, 35, 40, 45, 50 ($x10^{-6}$ mol L^{-1})

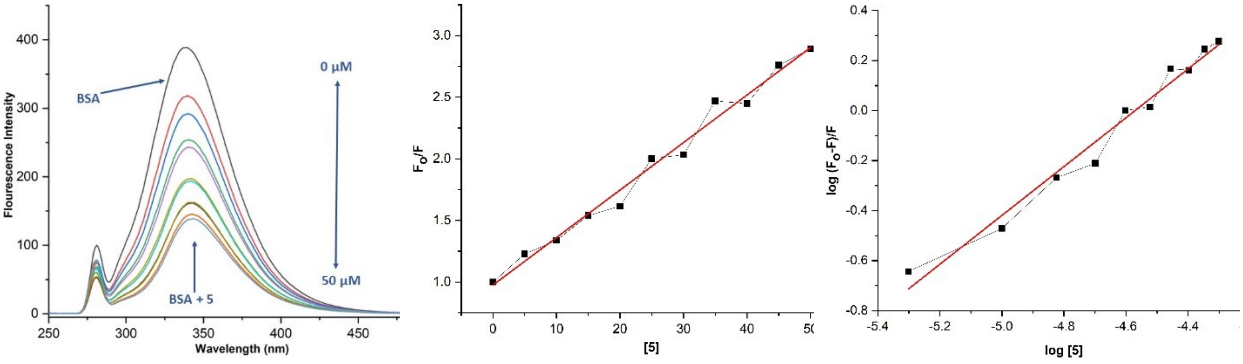

(a) **(b)** **(c)**

Fig. S27. (a) The fluorescence spectra of BSA with presence of **N2**, **(b)** Stern-Volmer plot of **N2** to BSA at 293 K, **(c)** The plot of log(F_0 −F)/F vs. log[**N2**] for quenching of **N2** to BSA (λex = 280 nm; λem = 338 nm. [BSA] = $1.00x10^{-5}$ mol L^{-1}, [**N2**] : 0, 5, 10, 15, 20, 25, 30, 35, 40, 45, 50 ($x10^{-6}$ mol L^{-1})

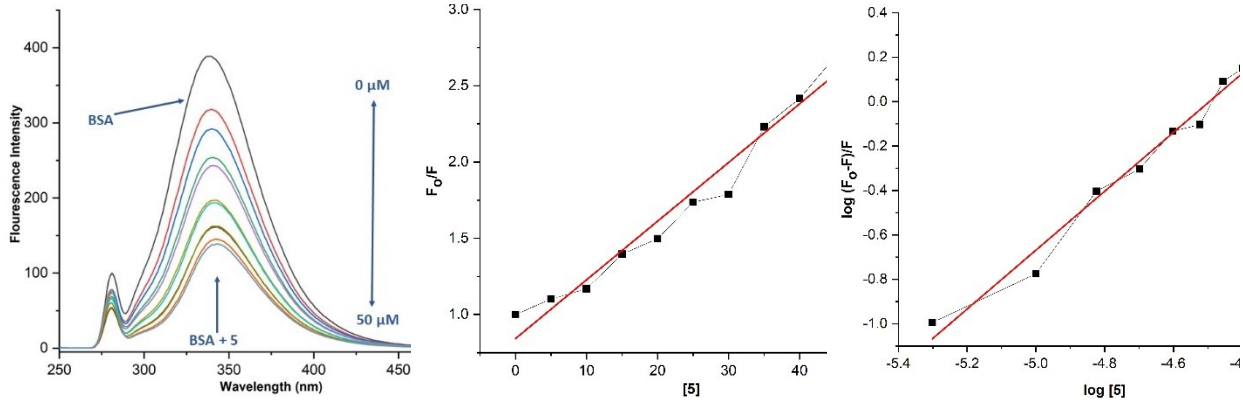

(a) **(b)** **(c)**

Fig. S28. (a) The fluorescence spectra of BSA with presence of **N2**, **(b)** Stern-Volmer plot of **N2** to BSA at 298 K, **(c)** The plot of log(F_0 −F)/F vs. log[**N2**] for quenching of **N2** to BSA (λex = 280 nm; λem = 338 nm. [BSA] = $1.00x10^{-5}$ mol L^{-1}, [**N2**] : 0, 5, 10, 15, 20, 25, 30, 35, 40, 45, 50 ($x10^{-6}$ mol L^{-1})

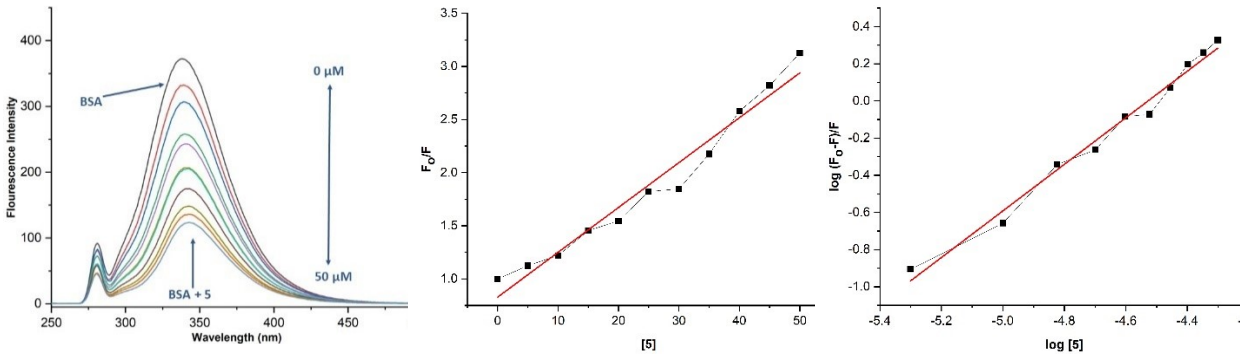

(a) **(b)** **(c)**

Fig. S29. (a) The fluorescence spectra of BSA with presence of **N2**, **(b)** Stern-Volmer plot of **N2** to BSA at 308 K, **(c)** The plot of log(F_0 −F)/F vs. log[**N2**] for quenching of **N2** to BSA (λex = 280 nm; λem = 338 nm. [BSA] = 1.00x10^{-5} mol L^{-1}, [**N2**] : 0, 5, 10, 15, 20, 25, 30, 35, 40, 45, 50 (x10^{-6} mol L^{-1})

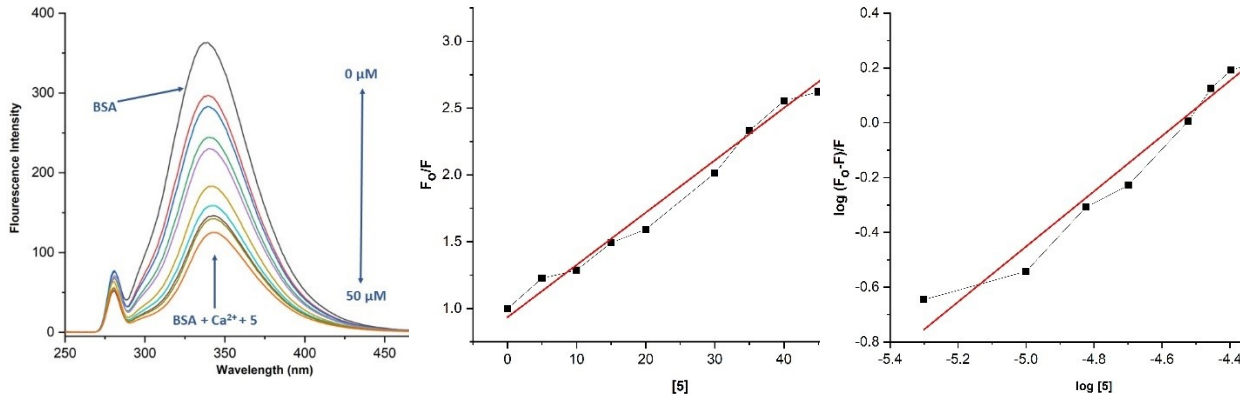

(a) **(b)** **(c)**

Fig. S30. (a) The fluorescence spectra of BSA with presence of **N2** and **Ca^{2+}** (1.00x10^{-5} mol L^{-1}), **(b)** Stern-Volmer plot of **N2** to BSA at 298 K with presence **Ca^{2+}**, **(c)** The plot of log(F_0 −F)/F vs. log[**N2**] for quenching of **N2** to BSA with presence **Ca^{2+}** (1.00x10^{-5} mol L^{-1}) (λex = 280 nm; λem = 338 nm. [BSA] = 1.00x10^{-5} mol L^{-1}, [**N2**] : 0, 5, 10, 15, 20, 25, 30, 35, 40, 45, 50 (x10^{-6} mol L^{-1})

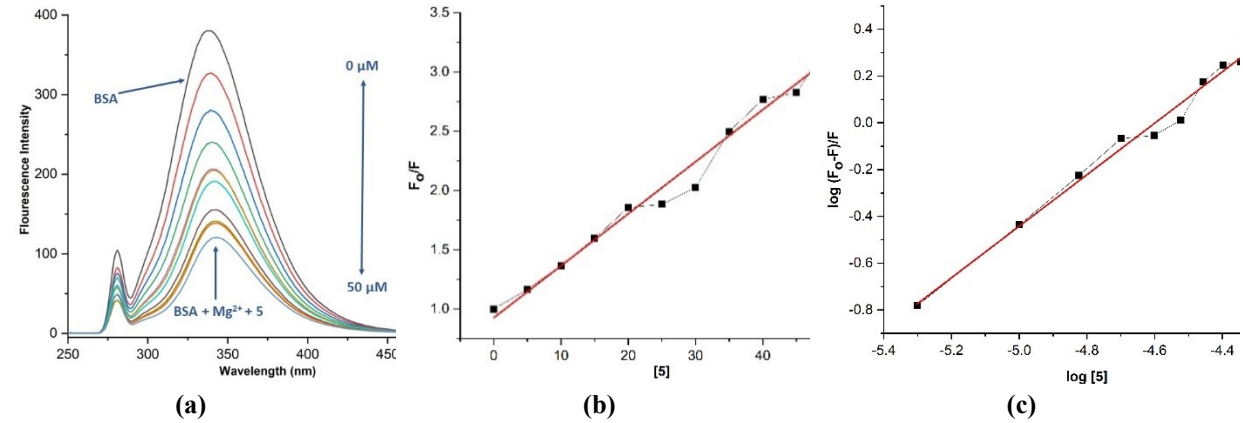

(a) **(b)** **(c)**

Fig. S31. (a) The fluorescence spectra of BSA with presence of **N2** and **Mg^{2+}** (1.00x10^{-5} mol L^{-1}), **(b)** Stern-Volmer plot of **N2** to BSA at 298 K with presence **Mg^{2+}**, **(c)** The plot of log(F_0 −F)/F vs. log[**N2**] for quenching of **N2** to BSA with presence **Mg^{2+}** (1.00x10^{-5} mol L^{-1}) (λex = 280 nm; λem = 338 nm. [BSA] = 1.00x10^{-5} mol L^{-1}, [**N2**] : 0, 5, 10, 15, 20, 25, 30, 35, 40, 45, 50 (x10^{-6} mol L^{-1}

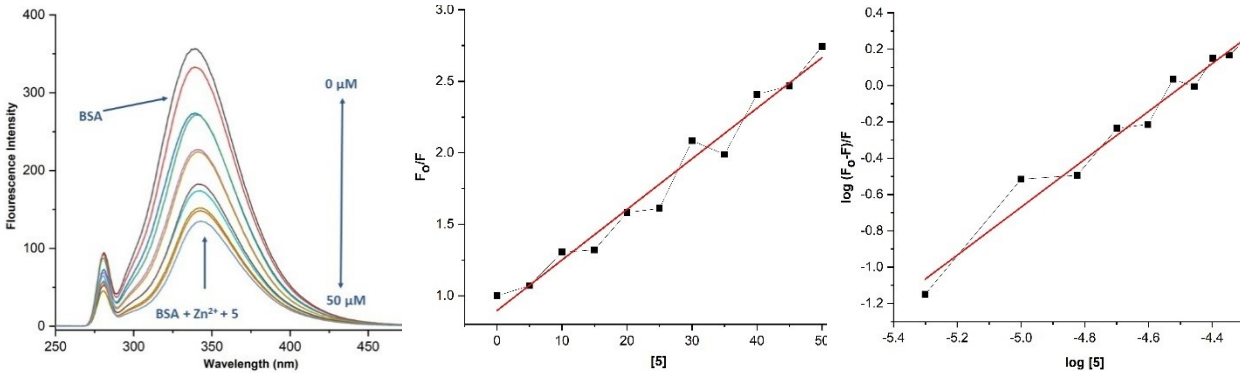

(a) **(b)** **(c)**

Fig. S32. (a) The fluorescence spectra of BSA with presence of **N2** and **Zn^{2+}** ($1.00x10^{-5}$ mol L^{-1}), **(b)** Stern-Volmer plot of **N2** to BSA at 298 K with presence **Zn^{2+}**, **(c)** The plot of log(F_0 −F)/F vs. log[**N2**] for quenching of **N2** to BSA with presence **Zn^{2+}** ($1.00x10^{-5}$ mol L^{-1}) (λex = 280 nm; λem = 338 nm. [BSA] = $1.00x10^{-5}$ mol L^{-1}, [**N2**] : 0, 5, 10, 15, 20, 25, 30, 35, 40, 45, 50 ($x10^{-6}$ mol L^{-1})

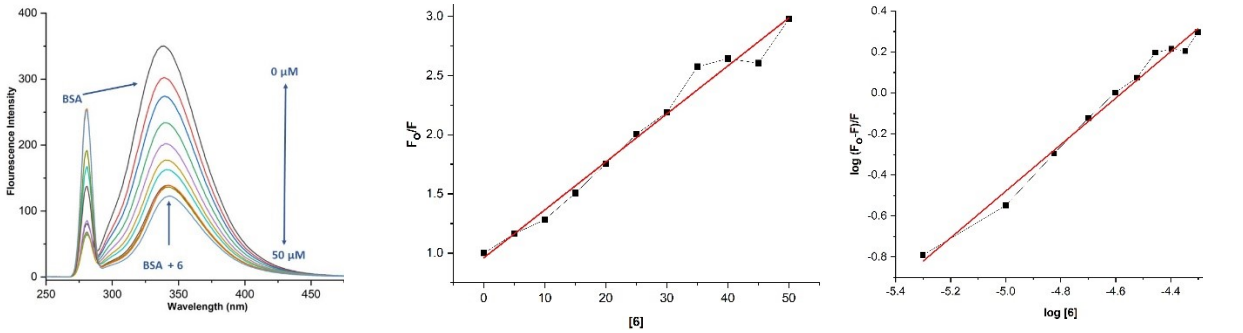

(a) **(b)** **(c)**

Fig. S33. (a) The fluorescence spectra of BSA with presence of **N3**, **(b)** Stern-Volmer plot of **N3** to BSA at 293 K, **(c)** The plot of log(F_0 −F)/F vs. log[**N3**] for quenching of **N3** to BSA (λex = 280 nm; λem = 338 nm. [BSA] = $1.00x10^{-5}$ mol L^{-1}, [**N3**] : 0, 5, 10, 15, 20, 25, 30, 35, 40, 45, 50 ($x10^{-6}$ mol L^{-1})

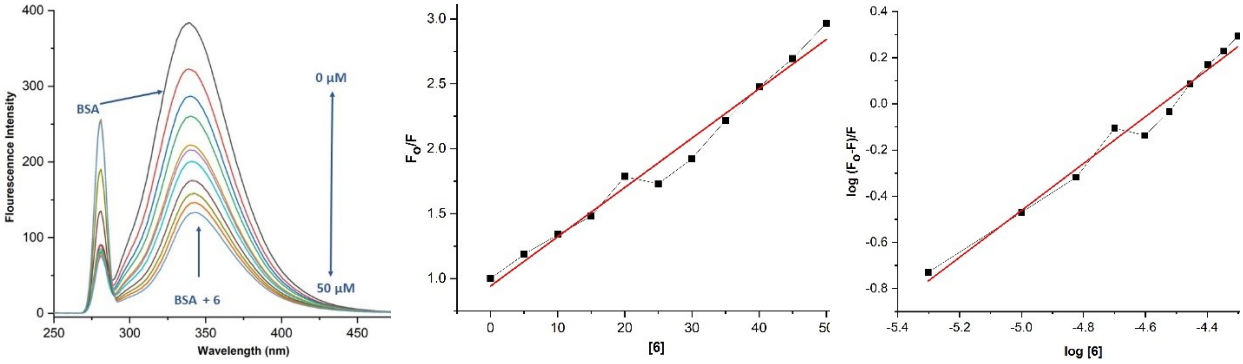

(a) **(b)** **(c)**

Fig. S34. (a) The fluorescence spectra of BSA with presence of **N3**, **(b)** Stern-Volmer plot of **N3** to BSA at 298 K, **(c)** The plot of log(F_0 −F)/F vs. log[**N3**] for quenching of **N3** to BSA (λex = 280 nm; λem = 338 nm. [BSA] = $1.00x10^{-5}$ mol L^{-1}, [**N3**] : 0, 5, 10, 15, 20, 25, 30, 35, 40, 45, 50 ($x10^{-6}$ mol L^{-1})

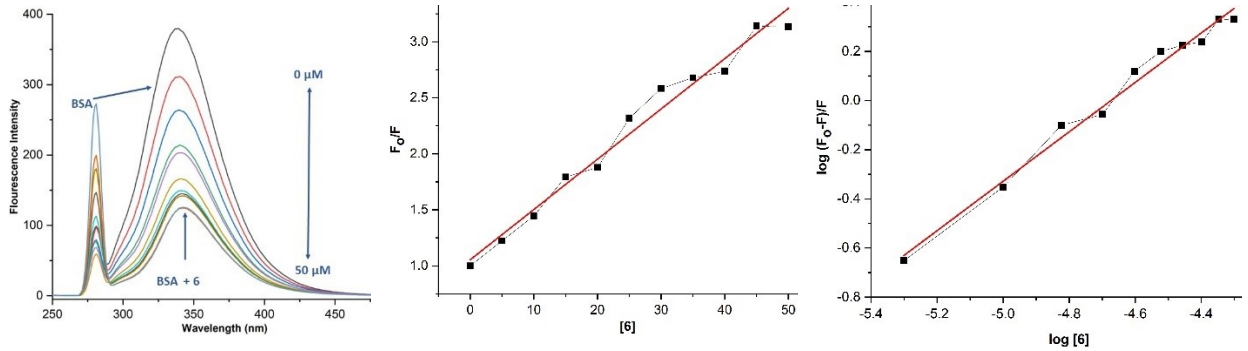

(a) **(b)** **(c)**

Fig. S35. (a) The fluorescence spectra of BSA with presence of **N3**, **(b)** Stern-Volmer plot of **N3** to BSA at 308 K, **(c)** The plot of log(F_0 −F)/F vs. log[**N3**] for quenching of **N3** to BSA (λex = 280 nm; λem = 338 nm. [BSA] = 1.00x10^{-5} mol L^{-1}, [**N3**] : 0, 5, 10, 15, 20, 25, 30, 35, 40, 45, 50 (x10^{-6} mol L^{-1})

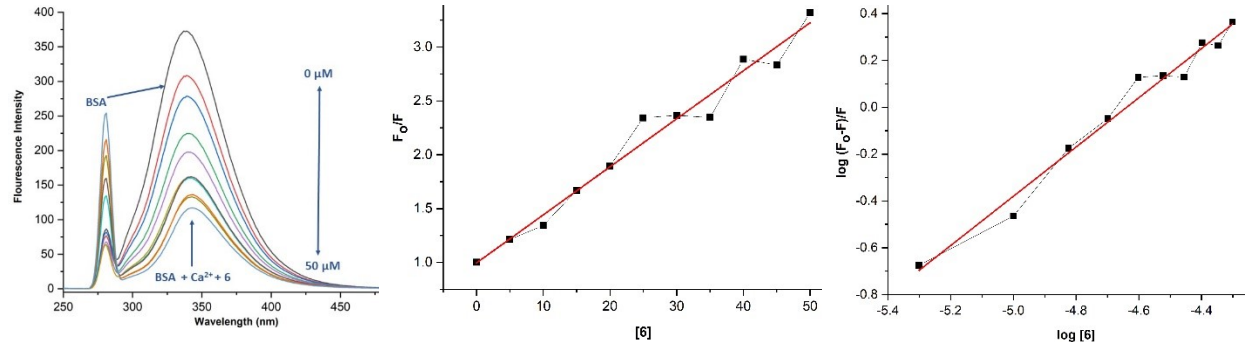

(a) **(b)** **(c)**

Fig. S36. (a) The fluorescence spectra of BSA with presence of **N3** and **Ca^{2+}** (1.00x10^{-5} mol L^{-1}), **(b)** Stern-Volmer plot of **N3** to BSA at 298 K with presence **Ca^{2+}**, **(c)** The plot of log(F_0 −F)/F vs. log[**N3**] for quenching of **N3** to BSA with presence **Ca^{2+}** (1.00x10^{-5} mol L^{-1}) (λex = 280 nm; λem = 338 nm. [BSA] = 1.00x10^{-5} mol L^{-1}, [**N3**] : 0, 5, 10, 15, 20, 25, 30, 35, 40, 45, 50 (x10^{-6} mol L^{-1})

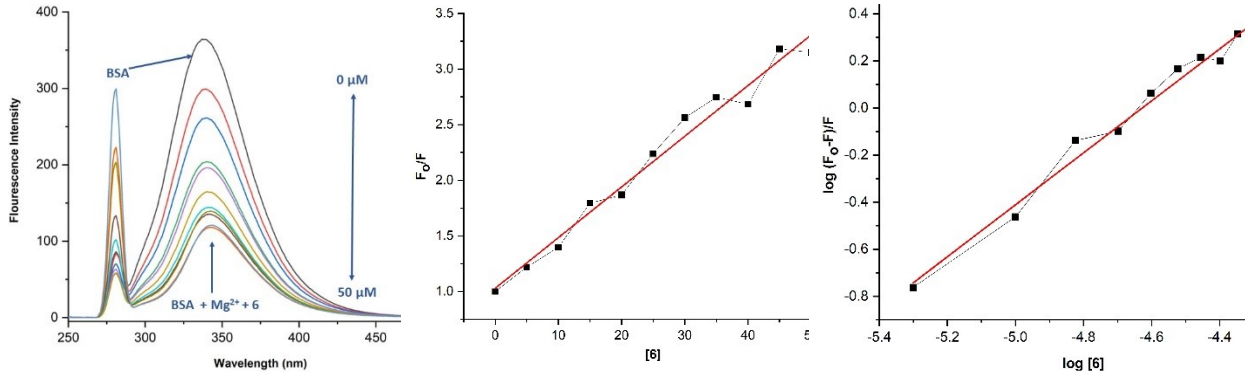

(a) **(b)** **(c)**

Fig. S37. (a) The fluorescence spectra of BSA with presence of **N3** and **Mg^{2+}** (1.00x10^{-5} mol L^{-1}), **(b)** Stern-Volmer plot of **N3** to BSA at 298 K with presence **Mg^{2+}**, **(c)** The plot of log(F_0 −F)/F vs. log[**N3**] for quenching of **N3** to BSA with presence **Mg^{2+}** (1.00x10^{-5} mol L^{-1}) (λex = 280 nm; λem = 338 nm. [BSA] = 1.00x10^{-5} mol L^{-1}, [**N3**] : 0, 5, 10, 15, 20, 25, 30, 35, 40, 45, 50 (x10^{-6} mol L^{-1})

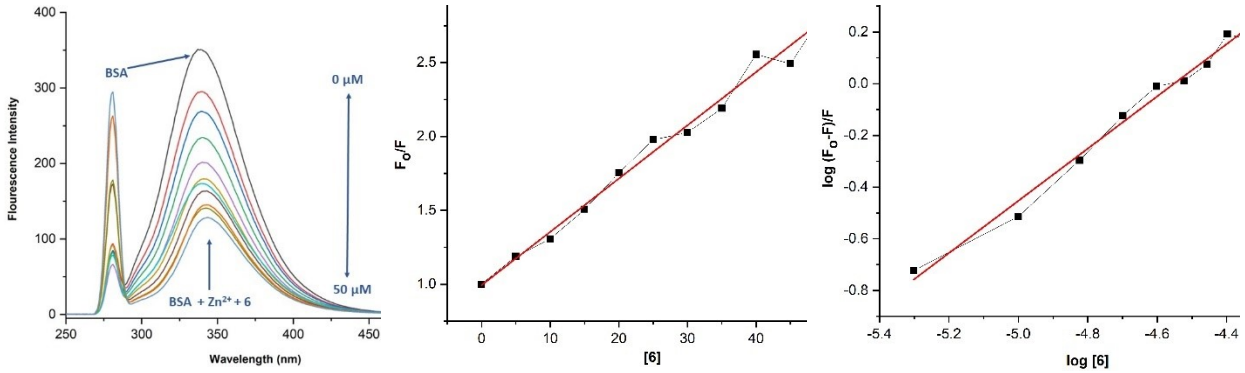

(a) **(b)** **(c)**

Fig. S38. (a) The fluorescence spectra of BSA with presence of **N3** and Mg^{2+} ($1.00x10^{-5}$ mol L^{-1}), **(b)** Stern-Volmer plot of **N3** to BSA at 298 K with presence Mg^{2+}, **(c)** The plot of $\log(F_0 - F)/F$ vs. log[**N3**] for quenching of **N3** to BSA with presence Mg^{2+} ($1.00x10^{-5}$ mol L^{-1}) (λex = 280 nm; λem = 338 nm. [BSA] = $1.00x10^{-5}$ mol L^{-1}, [**N3**] : 0, 5, 10, 15, 20, 25, 30, 35, 40, 45, 50 ($x10^{-6}$ mol L^{-1})

Table S4. NBO analysis results of the compounds, at B3LYP/6-311G(d,p) in gas

Donor(i)	ED_i/e	Acceptor (j)	ED_j/e	$E^{(2)}$/ kcalmol^{-1}	E(j)-E(i)/ a.u	F(i.j)/ a.u
C1						
π C6-C7	1.80143	π* C9-C10	0.28558	15.87	0.33	0.066
		π* C23≡N24	0.10661	20.05	0.39	0.081
π C9-C10	1.86219	π* C6-C7	0.43992	13.31	0.28	0.059
π C15-C16	1.66677	π* C13-O14	0.26765	11.55	0.30	0.053
		π* C17-C20	0.36997	20.67	0.28	0.068
		π* C18-C21	0.32386	18.62	0.29	0.066
π C17-C20	1.66610	π* C15-C16	0.37080	19.76	0.29	0.069
		π* C18-C21	0.32386	19.40	0.30	0.068
π C18-C21	1.64335	π* C15-C16	0.37080	22.88	0.28	0.071
		π* C17-C20	0.36997	21.86	0.27	0.069
LP (2) S8	1.62092	π* C6-C7	0.43992	27.06	0.25	0.074
		π* C9-C10	0.28558	18.99	0.29	0.068
LP (1) N11	1.65380	π* C6-C7	0.43992	38.32	0.29	0.096
		π* C13-O14	0.26765	45.93	0.31	0.109
LP (2) O14	1.84577	σ* C13-C15	0.06910	19.99	0.66	0.105
LP (3) *Cl*-15	1.91757	π* C17-C20	0.36997	13.25	0.32	0.063
C2						
π C6-C7	1.79982	π* C9-C10	0.28545	15.91	0.33	0.066
		π* C23≡N24	0.10739	20.17	0.39	0.081
π C9-C10	1.86116	π* C6-C7	0.44127	13.36	0.27	0.059
π C15-C16	1.65486	π* C13-O14	0.29572	18.20	0.28	0.065
		π* C17-C20	0.35392	21.41	0.28	0.069
		π* C18-C21	0.31411	19.51	0.29	0.067
π C17-C20	1.66361	π* C15-C16	0.37903	18.48	0.29	0.067
		π* C18-C21	0.31411	20.56	0.30	0.070
π C18-C21	1.64849	π* C15-C16	0.37903	21.16	0.28	0.069
		π* C17-C20	0.35392	20.33	0.28	0.067
LP (2) S8	1.62061	π* C6-C7	0.44127	27.12	0.25	0.074
		π* C9-C10	0.28545	18.97	0.29	0.068
LP (1) N11	1.65358	π* C6-C7	0.44127	38.42	0.29	0.096
		π* C13-O14	0.29572	52.05	0.29	0.112
LP (2) O14	1.85508	σ* C13-C15	0.06642	18.85	0.68	0.103
LP (3) *Cl*-15	1.92477	π* C17-C20	0.35392	12.46	0.33	0.062
C3						

π C6-C7	1.79977	π* C9-C10	0.28537	15.94	0.33	0.066
		π* C23≡N24	0.10768	20.22	0.39	0.081
π C9-C10	1.86182	π* C6-C7	0.44127	13.32	0.27	0.059
π C15-C16	1.65238	π* C13-O14	0.29873	19.00	0.28	0.066
		π* C17-C20	0.28693	20.09	0.29	0.070
		π* C18-C21	0.38431	20.37	0.27	0.067
π C17-C20	1.64859	π* C15-C16	0.38059	19.54	0.28	0.066
		π* C18-C21	0.38431	22.78	0.27	0.071
π C18-C21	1.66095	π* C15-C16	0.38059	20.08	0.30	0.070
		π* C17-C20	0.28693	17.84	0.30	0.067
LP (2) S8	1.62146	π* C6-C7	0.44127	27.10	0.25	0.074
		π* C9-C10	0.28537	18.94	0.29	0.068
LP (1) N11	1.65486	π* C6-C7	0.44127	38.55	0.29	0.096
		π* C13-O14	0.29873	52.07	0.29	0.112
LP (2) O14	1.85565	σ* C13-C15	0.06589	18.65	0.68	0.103
LP (3) *Cl*-15	1.91893	π* C18-C21	0.38431	13.25	0.33	0.063
N1						
π C6-C7	1.80346	π* C9-C10	0.28546	15.78	0.33	0.066
		π* C25≡N26	0.10548	19.89	0.39	0.081
π C9-C10	1.86201	π* C6-C7	0.43742	13.39	0.28	0.059
π C15-C16	1.65969	π* C13-O14	0.26255	4.05	0.32	0.033
		π* C17-C20	0.35693	20.47	0.28	0.068
		π* C18-C21	0.30551	20.12	0.29	0.069
π C17-C20	1.64993	π* C15-C16	0.33275	21.57	0.29	0.071
		π* C18-C21	0.30551	17.56	0.30	0.065
		π* N45-O47	0.61256	21.44	0.15	0.055
π C18-C21	1.63467	π* C15-C16	0.33275	20.23	0.28	0.068
		π* C17-C20	0.35693	23.17	0.28	0.072
LP (2) S8	1.61968	π* C6-C7	0.43742	27.12	0.25	0.074
		π* C9-C10	0.28546	19.03	0.29	0.068
LP (1) N11	1.65033	π* C6-C7	0.43742	37.45	0.29	0.095
		π* C13-O14	0.26255	46.46	0.32	0.111
LP (2) O14	1.83928	σ* C13-C15	0.07254	20.82	0.65	0.106
LP (2) O46	1.88924	σ* C17-N45	0.11057	12.54	0.56	0.075
		σ* N45-O47	0.05719	19.13	0.73	0.107
LP (2) O47	1.89425	σ* C17-N45	0.11057	13.99	0.56	0.079
		σ* N45-O46	0.06231	18.99	0.72	0.106
N2						
π C6-C7	1.80037	π* C9-C10	0.28502	15.77	0.33	0.066
		π* C24≡N25	0.10670	20.05	0.39	0.081
π C9-C10	1.85893	π* C6-C7	0.44145	13.55	0.27	0.059
π C15-C16	1.63799	π* C13-O14	0.29588	17.85	0.29	0.065
		π* C17-C20	0.33599	22.42	0.29	0.072
		π* C18-C21	0.29195	17.51	0.29	0.065
π C17-C20	1.63918	π* C15-C16	0.36093	17.80	0.29	0.064
		π* C18-C21	0.29195	21.68	0.29	0.073
		π* N45-O47	0.61452	22.79	0.15	0.057
π C18-C21	1.63092	π* C15-C16	0.36093	23.23	0.28	0.072
		π* C17-C20	0.33599	19.28	0.28	0.067
LP (2) S8	1.61827	π* C6-C7	0.44145	27.20	0.25	0.074
		π* C9-C10	0.28502	19.00	0.29	0.068
LP (1) N11	1.65356	π* C6-C7	0.44145	37.63	0.29	0.096
		π* C13-O14	0.29588	52.28	0.29	0.112
LP (2) O14	1.85417	σ* C13-C15	0.06799	19.20	0.67	0.103
LP (2) O46	1.89682	σ* C20-N45	0.11456	13.84	0.55	0.078
		σ* N45-O47	0.05487	18.64	0.73	0.105
LP (2) O47	1.89561	σ* C20-N45	0.11456	14.14	0.55	0.079
		σ* N45-O46	0.05570	18.84	0.73	0.106

N3						
π C6-C7	1.79972	π* C9-C10	0.28521	15.77	0.33	0.066
		π* C23≡N24	0.10568	19.90	0.39	0.081
π C9-C10	1.85741	π* C6-C7	0.44116	13.61	0.27	0.059
π C15-C16	1.63694	π* C13-O14	0.29737	17.05	0.28	0.063
		π* C17-C20	0.27040	18.47	0.29	0.067
		π* C18-C21	0.36561	21.12	0.28	0.070
π C17-C20	1.62622	π* C15-C16	0.36393	21.77	0.28	0.070
		π* C18-C21	0.36561	21.99	0.28	0.070
π C18-C21	1.63806	π* C15-C16	0.36393	19.10	0.29	0.067
		π* C17-C20	0.27040	19.23	0.30	0.070
		π* N45-O47	0.61911	25.28	0.15	0.059
LP (2) S8	1.61864	π* C6-C7	0.44116	27.08	0.25	0.074
		π* C9-C10	0.28521	19.01	0.29	0.068
LP (1) N11	1.65065	π* C6-C7	0.44116	37.67	0.29	0.096
		π* C13-O14	0.29737	52.54	0.29	0.112
LP (2) O14	1.85524	σ* C13-C15	0.06728	19.05	0.67	0.103
LP (2) O46	1.89665	σ* C21-N45	0.11310	13.84	0.56	0.079
		σ* N45-O47	0.05530	18.74	0.73	0.106
LP (2) O47	1.89655	σ* C21-N45	0.11310	13.84	0.56	0.079
		σ* N45-O46	0.05542	18.75	0.73	0.106

Table S5. The chemical reactivity values of the studied compounds

		H (-I)	L (-A)	ΔE	χ	η	ω (eV)	ω^+ (au)	ω^+ (au)	ΔN_{max}	$\Delta\varepsilon_{back\text{-}donat.}$
Chloroform	**C1**	-6.154	-1.880	4.274	-4.017	2.137	0.139	0.075	0.222	1.880	-0.534
	C2	-6.153	-2.119	4.035	-4.136	2.017	0.156	0.089	0.241	2.050	-0.504
	C3	-6.131	-2.084	4.047	-4.108	2.023	0.153	0.087	0.238	2.030	-0.506
	N1	-6.182	-2.908	3.275	-4.545	1.637	0.232	0.156	0.323	2.776	-0.409
	N2	-6.215	-2.950	3.265	-4.583	1.633	0.236	0.160	0.328	2.807	-0.408
	N3	-6.230	-3.144	3.086	-4.687	1.543	0.262	0.183	0.355	3.038	-0.386
Methanol	**C1**	-6.166	-1.900	4.267	-4.033	2.133	0.140	0.076	0.224	1.890	-0.533
	C2	-6.150	-2.109	4.040	-4.129	2.020	0.155	0.088	0.240	2.044	-0.505
	C3	-6.130	-2.078	4.052	-4.104	2.026	0.153	0.087	0.237	2.026	-0.506
	N1	-6.197	-2.937	3.260	-4.567	1.630	0.235	0.159	0.327	2.802	-0.408
	N2	-6.187	-2.957	3.231	-4.572	1.615	0.238	0.161	0.329	2.830	-0.404
	N3	-6.197	-3.135	3.061	-4.666	1.531	0.261	0.183	0.354	3.048	-0.383
DMSO	**C1**	-6.167	-1.901	4.266	-4.034	2.133	0.140	0.076	0.224	1.891	-0.533
	C2	-6.149	-2.108	4.041	-4.129	2.020	0.155	0.088	0.240	2.044	-0.505
	C3	-6.129	-2.077	4.052	-4.103	2.026	0.153	0.087	0.237	2.025	-0.507
	N1	-6.198	-2.939	3.259	-4.569	1.629	0.235	0.159	0.327	2.804	-0.407
	N2	-6.185	-2.957	3.229	-4.571	1.614	0.238	0.161	0.329	2.832	-0.404
	N3	-6.195	-3.134	3.060	-4.665	1.530	0.261	0.183	0.354	3.049	-0.383
	N1	-6.198	-2.941	3.257	-4.570	1.629	0.236	0.159	0.327	2.806	-0.407
	N2	-6.184	-2.957	3.226	-4.570	1.613	0.238	0.161	0.329	2.833	-0.403
	N3	-6.193	-3.134	3.059	-4.663	1.529	0.261	0.183	0.354	3.049	-0.382

Table S6. Active site analysis of crystal structure of SarA and BSA with the molecules (blue: H-bond, purple: pi-interactions, red: alkyl interactions, black: van der Waals interactions)

Molecules	BA*	Amino Acids Residue
		Bovine Serum Albumin
C1	-8.17	Ser192, Ser428, Arg458, His145, Ala193, Pro146, Arg196, Asp108, Tyr147, Phe148, Leu189, Thr190, Gln195, Glu424, Arg435, Leu454, Ile455
C2	-8.54	His145, Ser192, Ser428, Arg458, Ala193, Pro146, Phe148, Arg196, Asp108, Tyr147, Leu189, Thr190, Gln195, Arg435, Leu454, Ile455

C3	-7.06	His145, Ser428, Pro146, Tyr147, Leu189, Ala193, Arg196, Asp108, Phe148, Thr190, Ser192, Glu424, Lys431, Arg435, Ile455, Arg458
N1	-8.43	Leu189, Ser192, Arg458, Ala193, Pro146, Arg196, His145, Tyr147, Phe148, Thr190, Ser428, Arg435, Leu454, Ile455, Val461
N2	-8.84	Ser192, Ser428, Arg458, His145, Ala193, Pro146, Arg196, Asp108, Tyr147, Phe148, Tyr149, Leu189, Thr190, Gln195, Arg435, Leu454, Ile455
N3	-7.66	His145, Tyr148, Phe148, Arg196, Ser428, Ser192, Leu189, Ala193, Asp108, Arg144, Pro146, Thr190, Glu424, Lys431, Arg435, Ile455, Arg458
		Human Leukemia Inhibitory Factor
C1	-7.24	Val88, Gly96, Leu95, Ala120, Val89, Leu95, Ala120, Gly92, Thr93, Thr99, Arg100, Leu116, Asn117, Leu123, Leu127, Tyr147
C2	-7.29	Gly92, Thr93, Arg124, Leu95, Leu116, Ala120, Val88, Val89, Gly96, Thr99, Arg100, Asn117, Leu123, Leu127, Tyr147
C3	-7.13	Val88, Gly92, Arg124, Ala120, Val89, Thr93, Leu95, Gly96, Thr99, Arg100, Lys103, Asn117, Leu123, Leu127, Tyr147
N1	-7.90	Gly96, Arg124, Gly92, Ala120, Val88, Val89, Thr93, Leu95, Thr99, Arg100, Asn117, Leu123, Leu127, Tyr147
N2	-8.48	Gly92, Thr93, Arg100, Arg124, Ala120, Val88, Val89, Leu95, Gly96, Thr99, Lys103, Asn117, Leu123, Leu127, Tyr147
N3	-8.36	Gly96, Arg100, Lys103, Asn117, Arg124, Ala120, Val88, Val89, Gly92, Thr93, Leu95, Thr99, Leu123, Leu127, Tyr147

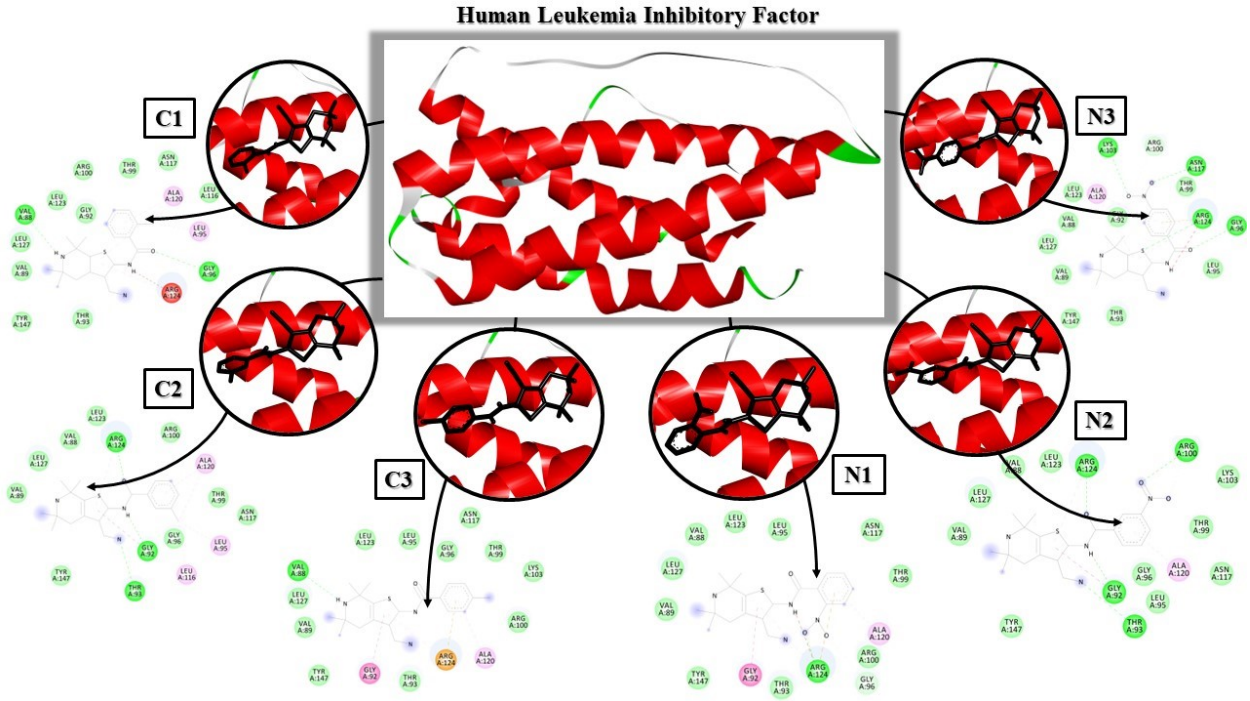

Fig. S39. Interaction residue in Human Leukemia Inhibitory Factor (middle), and interaction type of the molecules, (turquoise and green: H-bonds; fuchsia: pi-interactions; pink: alkylic interactions; pale green: van der Waals)

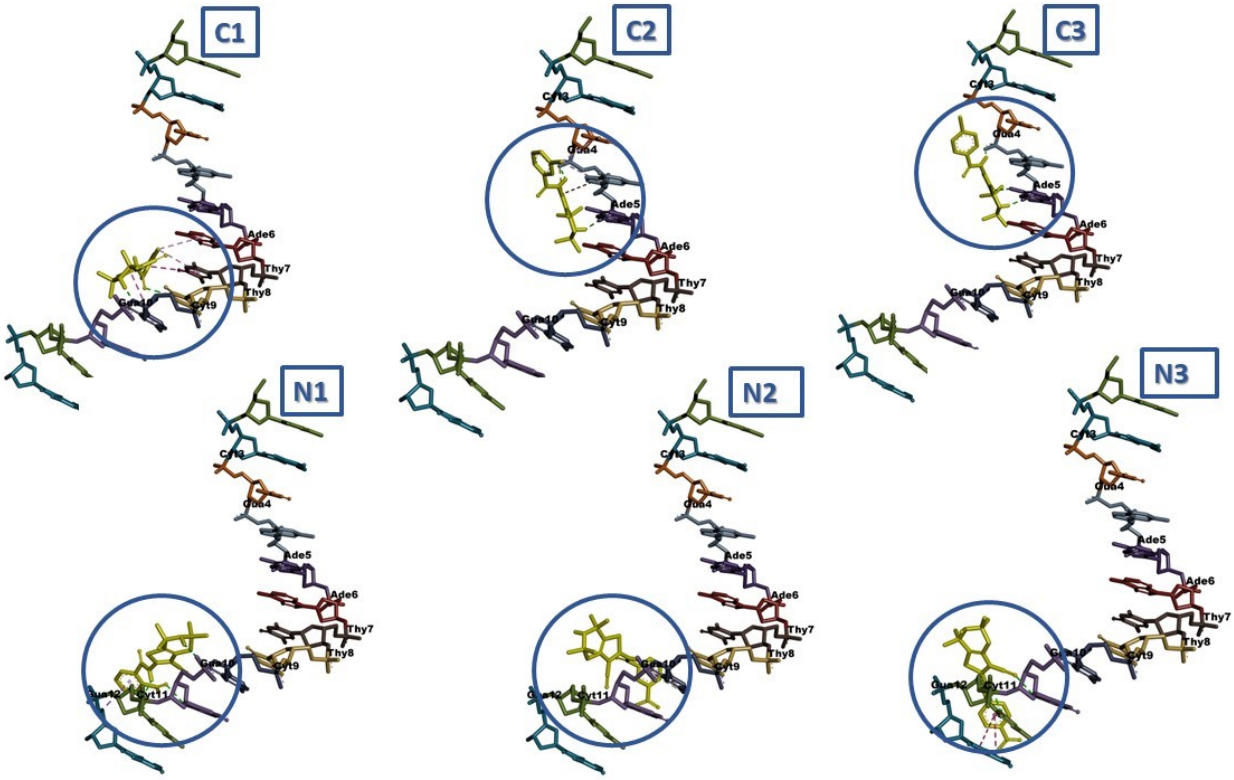

Fig. S40. Interaction residue in DNA dodecamer and interaction type of the molecules